Supporting Information for:

Protonophoric and mitochondrial uncoupling activity of aryl-carbamate substituted fatty acids.

Hugo MacDermott-Opeskin[1*], Callum Clarke[2*], Xin Wu[3,4], Ariane Roseblade[2], Edward York[2], Ethan Pacchini[2], Ritik Roy[2], Charles Cranfield[5], Philip A. Gale[3,6], Megan L. O'Mara[1,7], Michael Murray[8] and Tristan Rawling[2†]

[1] Research School of Chemistry, College of Science, The Australian National University, Canberra, ACT, 0200, Australia.

[2] School of Mathematical and Physical Sciences, Faculty of Science, University of Technology Sydney, Sydney, NSW, 2007, Australia.

[3] School of Chemistry, The University of Sydney, NSW, 2006, Australia.

[4] School of Chemistry and Molecular Biosciences, The University of Queensland, St Lucia, QLD 4072, Australia.

[5] School of Life Sciences, Faculty of Science, University of Technology Sydney, Sydney, NSW, 2007, Australia.

[6] The University of Sydney Nano Institute (SydneyNano), The University of Sydney, NSW, 2006, Australia.

[7] Australian Institute for Bioengineering and Nanotechnology, The University of Queensland, St Lucia, QLD 4072, Australia.

[8] Discipline of Pharmacology, School of Medical Sciences, The University of Sydney, NSW 2006, Australia.

*These authors contributed equally to this paper.

[†]Corresponding author

Table of Contents

1. Supplementary Figures: 3

2. Supplementary Tables: 10

3. Experimental Procedures- Chemistry 13

4. Experimental Procedures- Biology 20

5. Experimental Procedures- Tethered bilayer lipid membranes 22

6. Experimental Procedures- NMR Studies 23

5. Computational Methodology 24

6. Bibliography 26

7. ^{1}H and ^{13}C NMR spectra 29

8. Additional DFT data 41

1. Supplementary Figures:

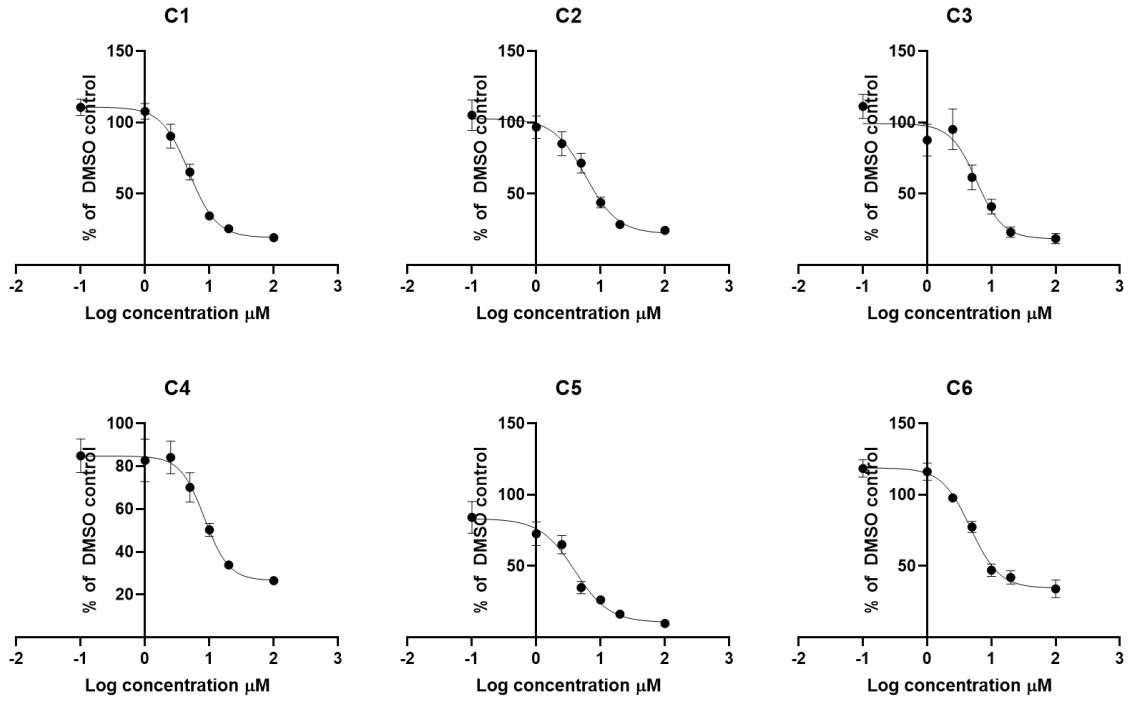

Figure S1 – Dose-response curves showing the effects of aryl-carbamates **C1-C6** on the JC-1 red:green fluorescence ratio in MDA-MB-231 breast cancer cells after 1 hour treatment with the test compound. Data represents the mean ± SEM from 3 independent experiments.

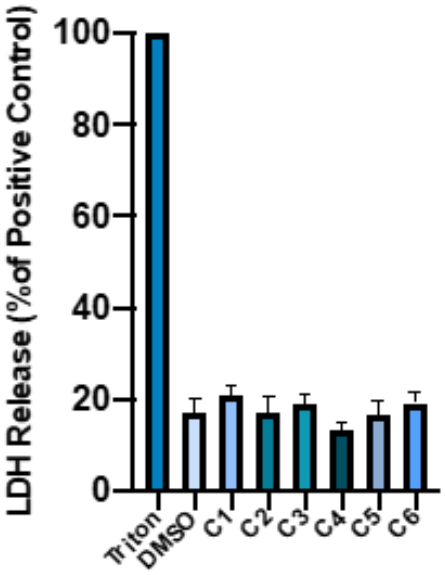

Figure S2 –LDH release by MDA-MB-231 cells treated with **C1** - **C6** (20 µM) for 48 hours. Values were standardized to positive control of 0.2% triton X100. Data represents the mean ± SEM from 3 independent experiments.

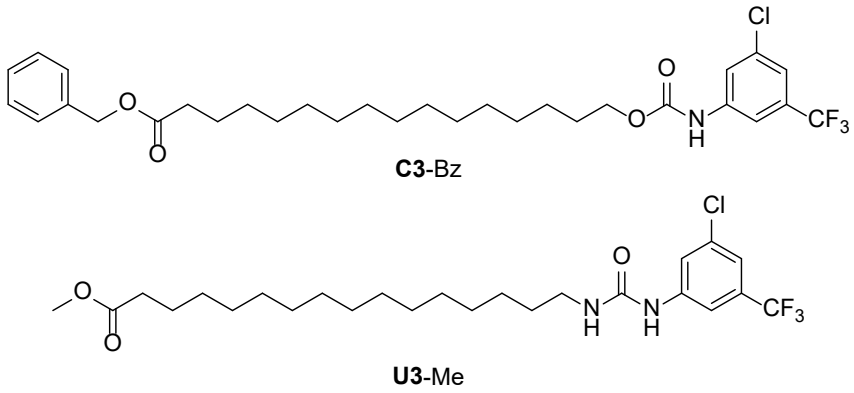

Figure S3. Structures of **C3** benzyl ester (**C3**-Bz) and **U3** methyl ester (**U3**-Me).

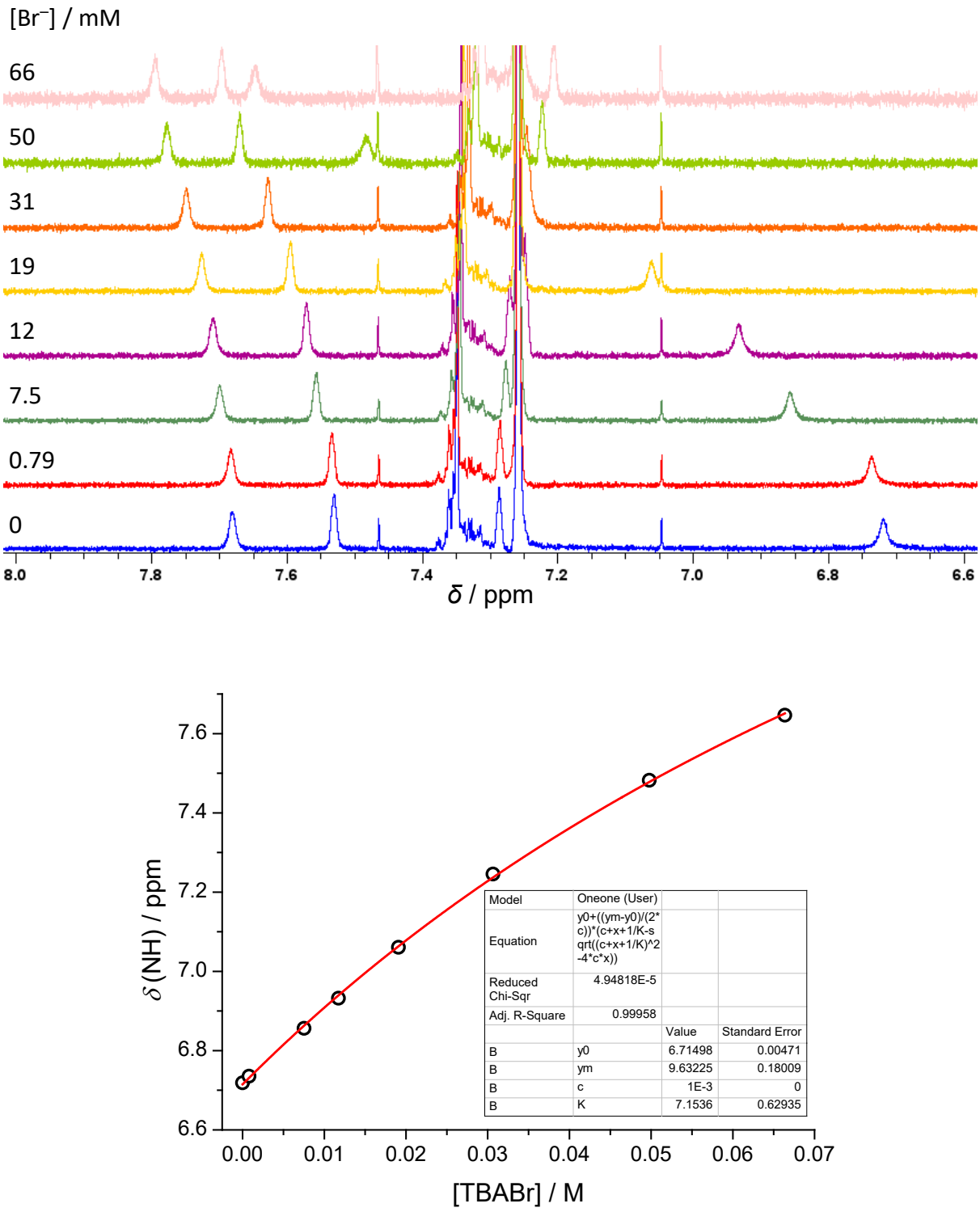

Figure S4. ^{1}H NMR (500 MHz) titration of a **C3**-Bz (1 mM) with TBABr in $CDCl_3$ at 298 K. The Br^- binding constant was determined to be 7.2 M^{-1} by fitting of the carbamate NH resonance (downfield shifted from 6.72 to 7.65 ppm with Br^- from 0 to 66 mM) to a 1:1 binding model.

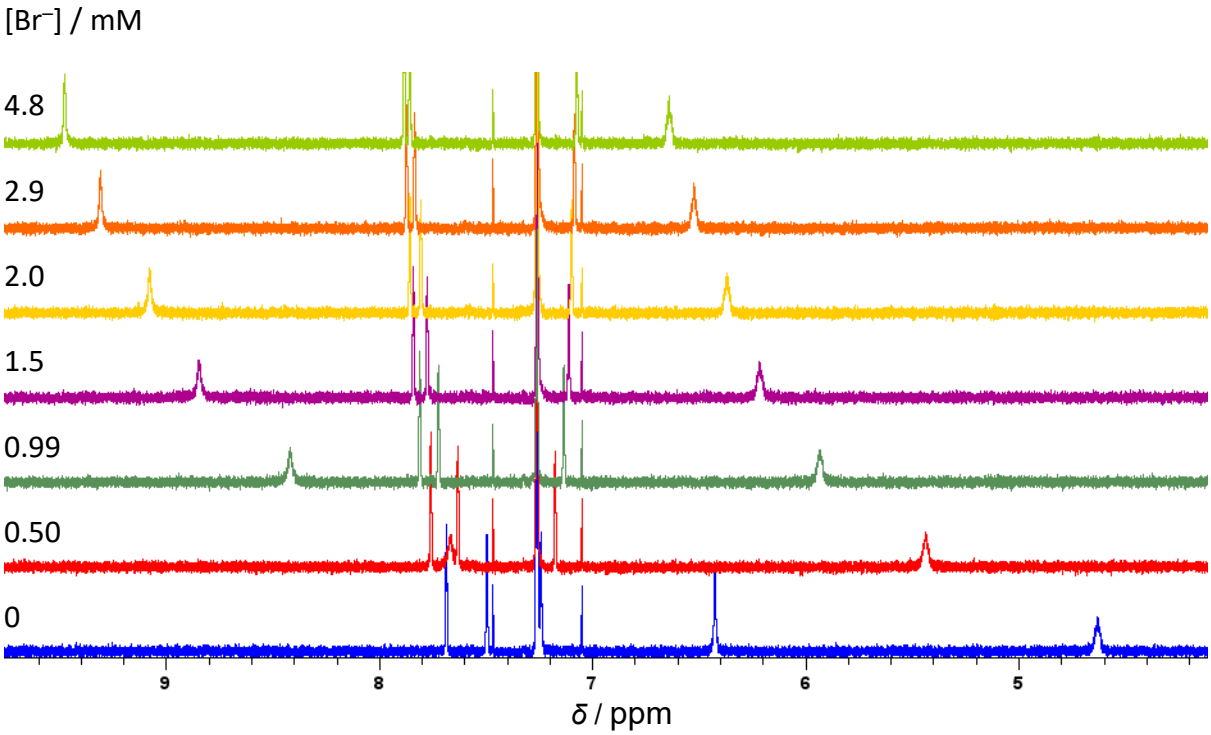

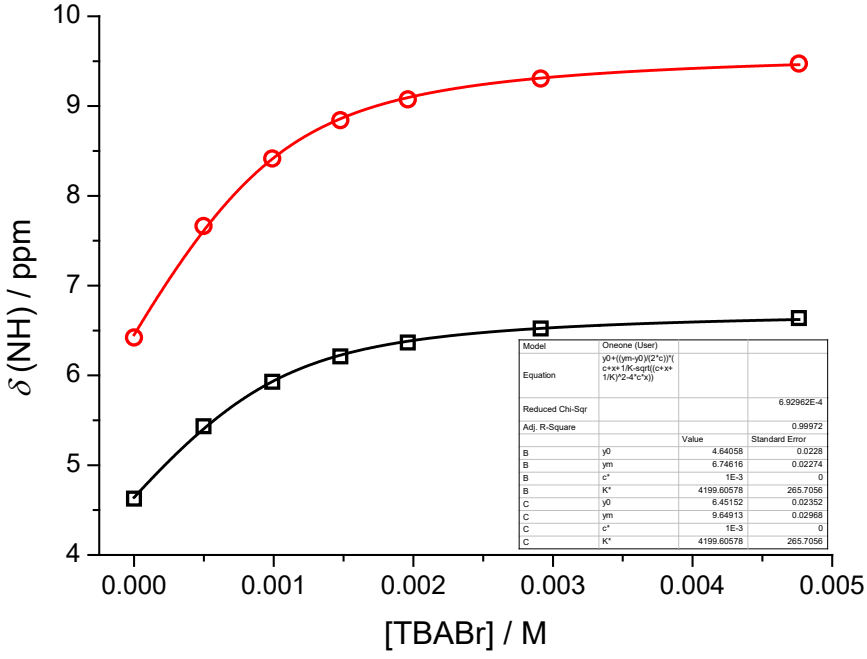

Figure S5. ^{1}H NMR (500 MHz) titration of a **U3**-Me (1 mM) with TBABr in $CDCl_3$ at 298 K. The Br^- binding constant was determined to be 4200 M^{-1} by global fitting of the two urea NH resonances to a 1:1 binding model.

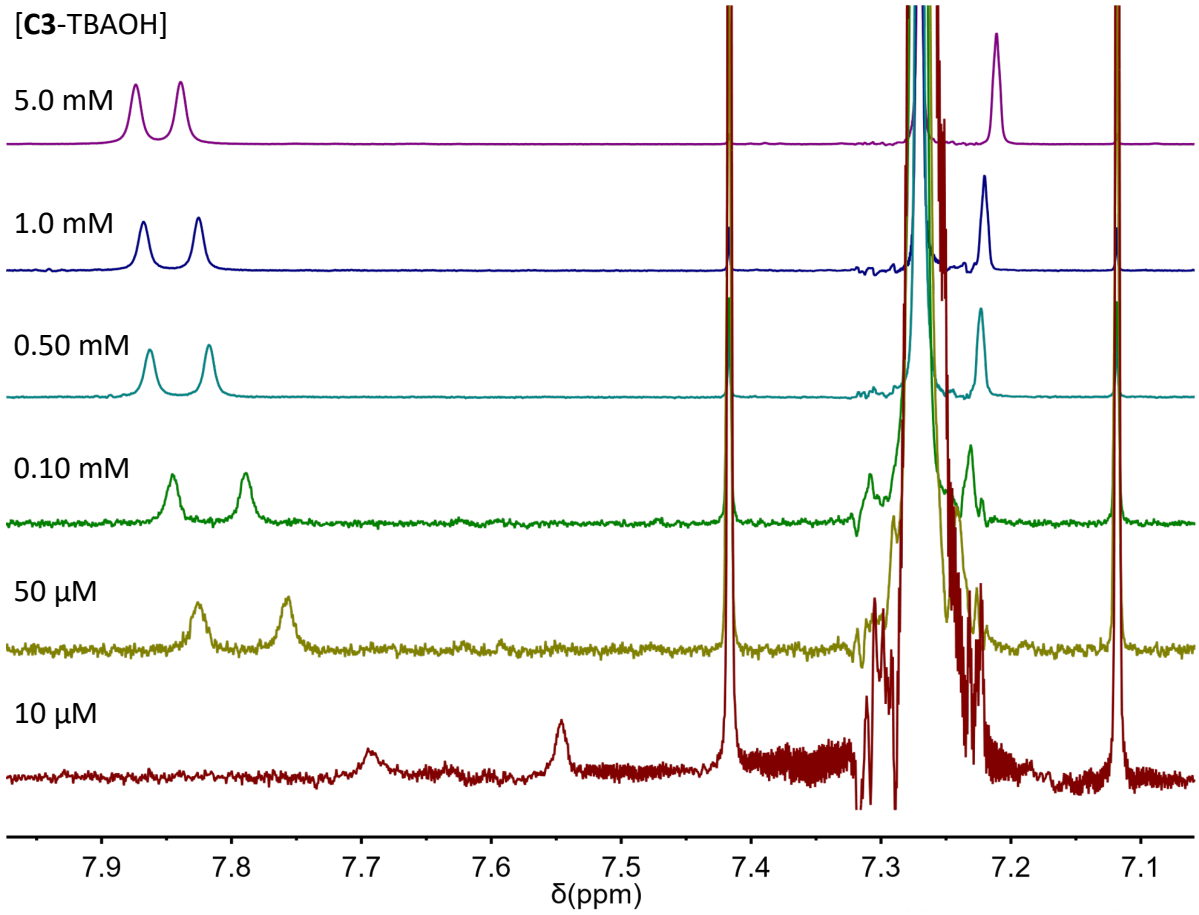

Figure S6. Concentration-dependent ^{1}H NMR (700 MHz) spectra of **C3**-TBAOH in $CDCl_3$ at 298 K. Note that the directions of shifting for the aromatic CH resonances upon increasing the **C3**-TBAOH concentration are identical to the trends observed upon titrating Br^- to **C3**-methyl ester (Figure S4). This is consistent with the hypothesis that **C3**-TBAOH forms intermolecular carbamate-carboxylate hydrogen bonds upon increasing the concentration.

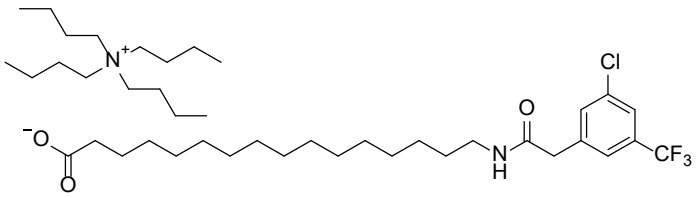

A3-TBAOH

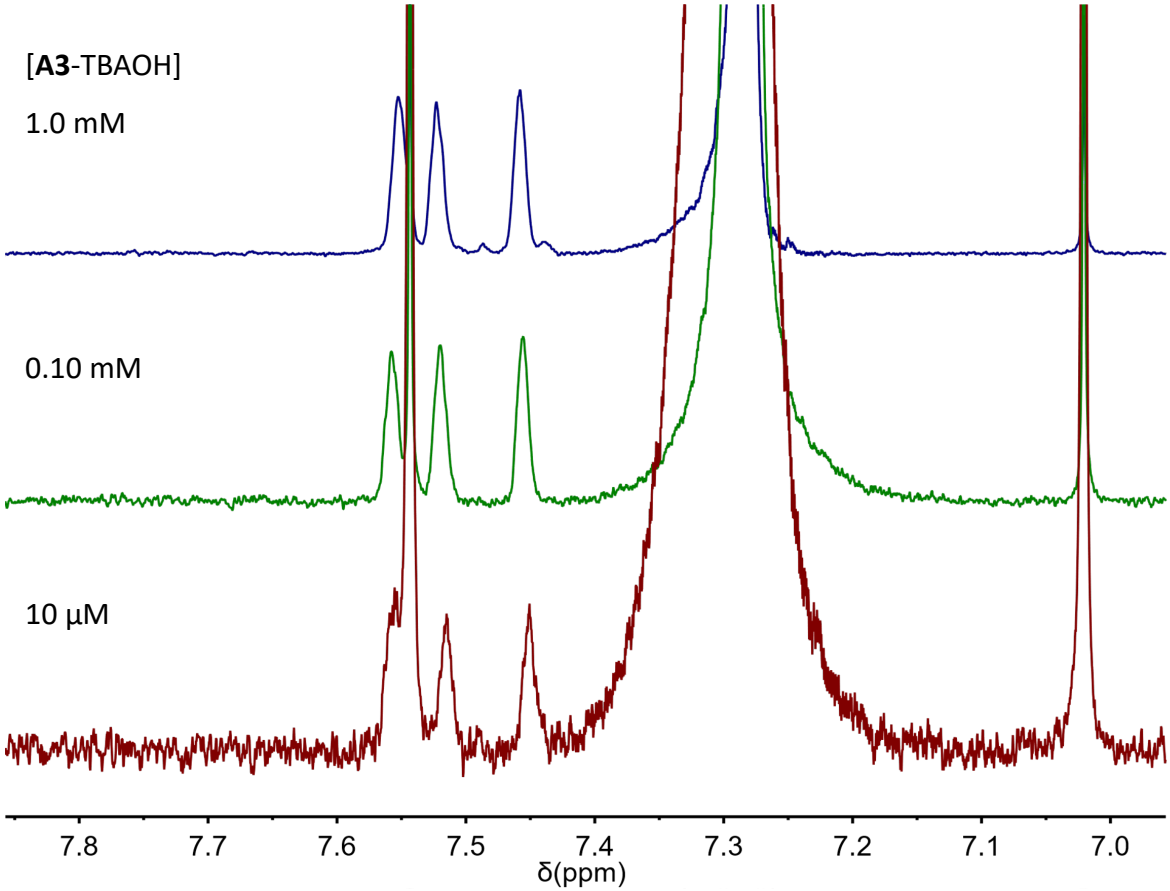

Figure S7. Concentration-dependent ^{1}H NMR (400 MHz) spectra of **A3**-TBAOH in $CDCl_3$ at 298 K. In contrast to **C3**-TBAOH, no chemical shift changes were observed for **A3**-TBAOH after 100-fold dilution, indicating no aggregation of **A3**-TBAOH.

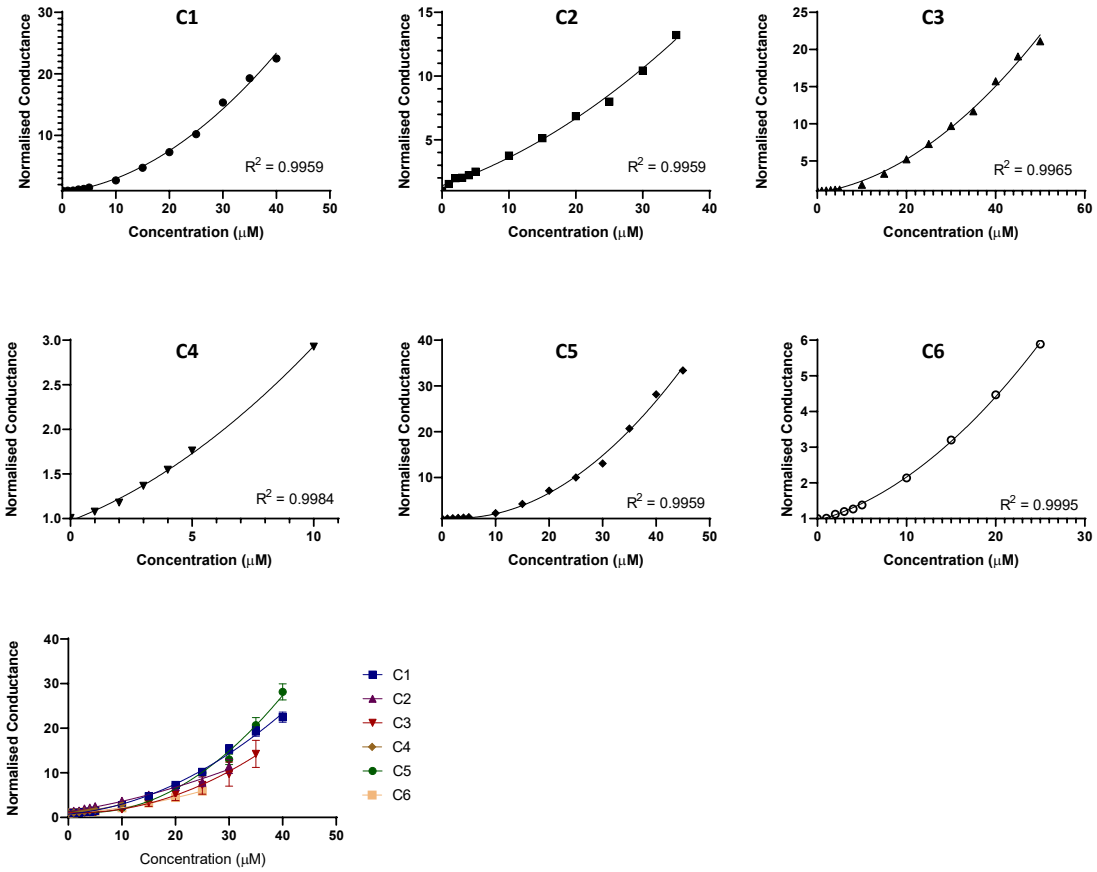

Figure S8 – Conductance measures of DOPC tethered bilayer lipid membranes in response to increasing concentrations of aryl-carbamates **C1** – **C6**. In panel (a) each carbamate is plotted individually, and in panel (b) **C1**-**C6** are plotted on the same set of axes for comparison. Quadratic regressions were made with GraphPad Prism 8.2.1. Data represents the mean of three independent experiments.

2. Supplementary Tables:

Table S1 Comparison of diffusion coefficients of **U3**-TBAOH, **C3**-TBAOH and **A3**-TBAOH in $CDCl_3$ at 298 K, determined by diffusion NMR based on two aromatic CH peaks.

Compound	*D* / (10^{-9} m^2/s)		
	ArH1	ArH2	Average ± SD
U3-TBAOH (5 mM)	1.12	1.05	1.09 ± 0.05
C3-TBAOH (5 mM)	1.21	1.22	1.22 ± 0.01
A3-TBAOH (5 mM)	1.49	1.52	1.51 ± 0.03

Table S2: Propanoate binding affinities of compounds in **Table 1** at the DSD-PBE-P86/aug-cc-pVTZ // M06-2X-D3(0)/6-311+G(d) level of theory. Components of these energies can be found in **Table S5** (Additional data)

Compound	**Propanoate binding enthalpy (kJ/mol)** M06-2X-D3(0)/6-311+G(d)//DSD-PBE-P86/aug-cc-pVTZ		
	Gas	**Water**	**n-Pentadecane**
C1	-98.70	20.57	-49.30
C2	-107.25	6.14	-57.28
C3	-99.60	7.09	-51.22
C4	-117.27	10.75	-62.51
C5	-112.67	7.42	-60.80
C6	-112.02	7.87	-59.09
U1	-154.41	11.06	-89.39
U2	-159.44	8.74	-95.02
U3	-153.73	10.24	-90.13
U4	-175.09	4.51	-104.82
U5	-163.64	10.71	-96.62
U6	-163.92	7.46	-98.44

Table S3: Calculated Lop P (cLog P) values of the aryl-urea and aryl-carbamate substituted fatty acids

	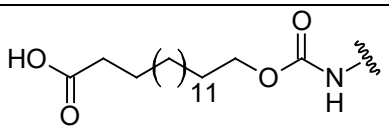 **Carbamate series**		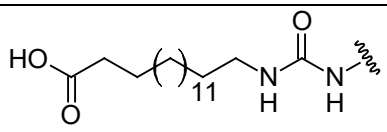 **Urea series**	
R	**Compound**	**cLog P ± SD[a]**	**Compound**	**cLog P ± SD[a]**
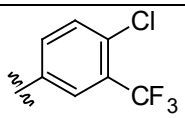	**C1**	7.85 ± 0.47	**U1**	7.17 ± 0.47
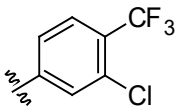	**C2**	7.85 ± 0.47	**U2**	7.17 ± 0.47
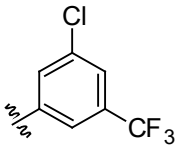	**C3**	7.85 ± 0.47	**U3**	7.17 ± 0.47
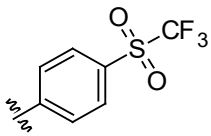	**C4**	7.25 ± 0.47	**U4**	6.57 ± 0.47
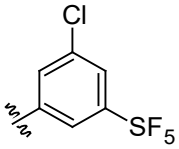	**C5**	n.c[b]	**U5**	n.c[b]
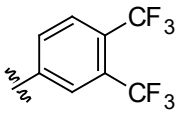	**C6**	8.22 ± 0.47	**U6**	7.62 ± 0.47

[a] cLog P values calculated in ChemDraw Ultra 12 using Crippen's Fragmentation.

[b] cLog P could not be calculated

Table S4: NPA charges on the carboxylate moiety of compounds in **Table 1** at the DSD-PBE-P86/aug-cc-pVTZ level of theory

Compound Number	**NPA charge on propanoate moiety**	
	Carbamate (C)	**Urea (U)**
1	-0.912	-0.898
2	-0.908	-0.894
3	-0.899	-0.893
4	-0.900	-0.888
5	-0.895	-0.890
6	-0.906	-0.888

3. Experimental Procedures- Chemistry

General Chemistry

10 was prepared according to literature procedure.[25] All reagents and anhydrous reagents were purchased from Sigma Aldrich (Castle Hill, NSW, Australia) or Flurochem (Hadfield, Derbyshire, United Kingdom) and used without further purification. TLC was performed on silica gel 60 F254 plates. TLC plates were visualised with UV light and potassium permanganate TLC stain. Dry Column Vacuum Chromatography (DCVC) was used to purify reaction products on silica gel with gradient elutions. ^{1}H and ^{13}C NMR spectra were recorded on an Agilent 500 MHz NMR. Spectra were referenced internally to residual solvent ($CDCl_3$; ^{1}H δ 7.26, ^{13}C δ 77.10. DMSO-*d*$_6$; ^{1}H δ 2.49, ^{13}C δ 39.52. Acetone-*d*$_6$; ^{1}H δ 2.09, ^{13}C δ 206.26). High resolution mass spectrometry (HRMS) was performed on an Agilent Technologies 6510 Q-TOF LCMS. Melting points were measured on a Stuart SMP10 melting point apparatus. The purity of all test compounds was determined to be ≥ 95% by absolute quantitative ^{1}H NMR spectroscopy using 1,3,5-trioxane as the internal calibrant (see *J. Med. Chem*. **2014**, 57, 9219-9219 for full procedure)

Benzyl 16-Hydroxyhexadecanoate (2).

16-hydroxyhexadecanoic acid (11.24 mmol) was dissolved in anhydrous dimethylformamide (50 mL) under a nitrogen atmosphere. Cs_2CO_3 (21.91 mmol) and benzyl bromide (13.45 mmol) were added to the solution, which was left to stir at 60^{o}C for 18 h. Water was added to the solution (100 mL) and extracted with ethyl acetate (3 x 100 mL). Combined organic extracts were washed with water (2 x 200 mL), brine (1 x 200 mL) and dried on Mg_2SO_4. The solution was then concentrated under reduced pressure. The crude residue was purified by DCVC using gradient elutions of dichloromethane/ethyl acetate (100:0 to 80:20), yielding **3** as a pure white solid. 71% yield. (500 MHz, $CDCl_3$): δ 7.35-7.30 (m, 5H), 5.10 (s, 2H), 3.60 (t, *J* = 7.0 Hz, 2H), 2.35 (t, *J* = 7.5 Hz, 2H), 1.70-1.40 (m, 4H), 1.35-1.25 (m, 22H). ^{13}C NMR (125 MHz, $CDCl_3$): δ 173.6, 136.0, 128.6 (2C), 128.0 (2C), 66.1, 63.0, 34.3, 32.6, 29.6, 29.4 (2C), 29.3, 29.2, 29.1, 29.0 (2C), 28.8, 28.7, 25.0, 24.9. HRMS (ESI) *m/z* $[M+H]^+$ calcd for $C_{23}H_{38}O_3$, 363.2893; found 363.2895.

General procedure A: Carbamate formation

To a solution of the appropriately substituted aniline (1.65 mmol) in anhydrous dichloromethane (7 mL) under nitrogen atmosphere was added *N,N*-carbonyldiimidazole (2.06 mmol). The solution was left to stir at room temperature for 2h. 16-Hydroxyhexadecanoic acid benzyl ester (1.37 mmol) was added to the reaction, and was then stirred at room temperature for 18 h. The solution was diluted with ethyl acetate (50 mL) and washed with water (2 x 100 mL), brine (1 x 100 mL) and dried on Mg_2SO_4. The solution was then concentrated under reduced pressure. The residue was purified by DCVC using gradient elutions with hexane/dichloromethane (25:75 to 0:100).

Benzyl 16-(((4-chloro-3-(trifluoromethyl)phenyl)carbamoyl)oxy)hexadecanoate (3).

White solid, 36% yield. ^{1}H NMR (500 MHz, $CDCl_3$): δ 7.73 (s, 1H), 7.56-7.55 (d, *J* = 7.5 Hz, 1H), 7.43-7.41 (d, *J* = 9 Hz, 1H), 7.36-7.30 (m, 5H), 6.70 (s, 1H), 5.11 (s, 2H), 4.19-4.16 (t, *J* = 6.5 Hz, 2H), 2.35 (t, *J* = 8 Hz, 2H), 1.70-1.61 (m, 4H), 1.37-1.25 (m, 22H). ^{13}C NMR (125 MHz, $CDCl_3$): δ 173.9, 153.4, 137.1, 136.2, 132.0, 129.0 (q, *J* = 31 Hz), 128.6 (2C), 128.2 (3C), 125.9, 122.6 (q, *J* = 273 Hz), 122.4, 117.6, 66.2, 66.1, 34.4, 29.7 (3C), 29.7, 29.6, 29.6, 29.5, 29.3 (2C), 29.2, 28.9, 25.9, 25.1. HRMS (ESI) *m/z* $[M+H]^+$ calcd for $C_{31}H_{42}ClF_3NO_4$, 584.2749; found, 584.2744.

Benzyl 16-(((3-chloro-4-(trifluoromethyl)phenyl)carbamoyl)oxy)hexadecanoate (4).

White solid, 19% yield. ^{1}H NMR (500 MHz, $CDCl_3$): δ 7.66 (s, 1H), 7.60-7.58 (d, *J* = 8.5 Hz), 7.36-7.32 (m, 6H), 6.89 (s, 1H), 5.12 (s, 2H), 4.19-4.17 (t, *J* = 7.0 Hz, 2H), 2.37-2.34 (t, *J* = 7.5 Hz, 2H), 1.69-1.62 (m, 4H), 1.39-1.28 (m, 22H). ^{13}C NMR (125 MHz, $CDCl_3$): δ 173.9, 153.1, 142.1, 136.2, 133.3, 128.6 (2C), 128.3 (q, *J* = 6 Hz), 128.26, 128.2 (2C), 123.0 (q, *J* = 273 Hz), 122.8 (q, *J* = 31 Hz), 120.4, 115.7, 66.19, 66.17, 34.5, 29.69 (3C), 29.65, 29.63, 29.59, 29.51, 29.3 (2C), 29.2, 28.9, 25.9, 25.1. HRMS (ESI) *m/z* $[M+H]^+$ calcd for $C_{31}H_{42}ClF_3NO_4$, 584.2749; found, 584.2760.

Benzyl 16-(((3-chloro-5-(trifluoromethyl)phenyl)carbamoyl)oxy)hexadecanoate (5).

White solid, 66% yield. ^{1}H NMR (500 MHz, $CDCl_3$): δ 7.68 (s, 1H), 7.54 (s, 1H), 7.36-7.31 (m, 5H), 7.29 (s, 1H), 6.79 (s, 1H), 5.11 (s, 2H), 4.19-4.17 (t, *J* = 6.5 Hz, 2H), 2.37-2.34 (t, *J* = 7.5 Hz, 2H), 1.70-1.61 (m, 4H), 1.39-1.28 (m, 22H). ^{13}C NMR (125 MHz, $CDCl_3$): δ 173.9, 153.2, 139.9, 136.2, 135.6, 132.8 (q, *J* = 31 Hz), 128.6 (2C), 128.2 (3C), 122.1 (q, *J* = 273 Hz), 121.5, 120.1,

113.4, 66.1 (2C), 34.4, 29.68 (3C), 29.64, 29.62, 29.58, 29.51, 29.3 (2C), 29.2, 28.9, 25.9, 25.0. HRMS (ESI) *m/z* $[M+H]^+$ calcd for $C_{31}H_{42}ClF_3NO_4$, 584.2749; found, 584.2759.

Benzyl 16-(((4-((trifluoromethyl)sulfonyl)phenyl)carbamoyl)oxy)hexadecanoate (6).

White solid, 39% yield. ^{1}H NMR (500 MHz, $CDCl_3$): δ 7.95-7.93 (m, 2H), 7.72-7.70 (m, 2H), 7.42-7.31 (m, 6H), 5.12 (s, 2H), 4.21-4.19 (t, *J* = 7.0 Hz, 2H), 2.38-2.35 (t, *J* = 7.5 Hz, 2H), 1.71-1.61 (m, 4H), 1.39-1.25 (m, 22H). ^{13}C NMR (125 MHz, $CDCl_3$): δ 174.0, 153.0, 146.2, 132.4 (2C), 128.5 (2C), 128.2 (2C), 128.1 (2C), 123.7, 119.9 (q, *J* = 325 Hz), 118.4, 118.3, 66.3, 66.2, 34.4, 29.59 (3C), 29.54, 29.53, 29.49, 29.42, 29.2 (2C), 29.1, 28.8, 25.8, 25.0. HRMS (ESI) *m/z* $[M+H]^+$ calcd for $C_{31}H_{43}F_3NO_6S$, 614.2758; found, 614.2748.

Benzyl 16-(((3-chloro-5-(pentafluoro-λ^6-sulfaneyl)phenyl)carbamoyl)oxy)hexadecanoate (7).

White solid, 26% yield. ^{1}H NMR (500 MHz, $CDCl_3$): δ 7.69 (s, 2H), 7.42 (s, 1H), 7.35-7.30 (m, 5H), 6.76 (s, 1H), 5.11 (s, 2H), 4.20-4.17 (t, *J* = 7.0 Hz, 2H), 2.37-2.34 (t, *J* = 7.5 Hz, 2H), 1.69-1.62 (m, 4H), 1.35-1.25 (m, 22H). ^{13}C NMR (125 MHz, $CDCl_3$): δ 173.9, 154.6 (t, *J* = 19 Hz), 153.2, 139.5, 136.2, 134.1, 128.6 (2C), 128.4 (2C), 128.2, 121.4, 120.9, 114.4, 66.3, 66.2, 34.5, 29.67 (3C) 29.64, 29.61, 29.57, 29.50, 29.3 (2C), 29.2, 29.0, 25.9, 25.1. HRMS (ESI) *m/z* $[M+H]^+$ calcd for $C_{30}H_{42}ClF_5NO_4S$, 642.2438; found, 642.2436.

Benzyl 16-(((3,4-bis(trifluoromethyl)phenyl)carbamoyl)oxy)hexadecanoate (8).

White solid, 11% yield. ^{1}H NMR (500 MHz, $CDCl_3$): δ 8.87 (s, 1H), 7.80 – 7.65 (m, 2H), 7.40 – 7.30 (m, 5H), 5.17 (s, 2H), 4.21 (t, *J* = 7.0 Hz, 2H), 2.18 (t, *J* = 7.5 Hz, 2H), 1.70 – 1.60 (m, 4H), 1.42 – 1.20 (m, 22H).^{13}C NMR (125 MHz, $CDCl_3$): 174.0, 153.2, 141.7, 136.2, 129.3 (p, *J* = 6 Hz), 128.6 (2C), 128.3, 128.2 (2C), 126.0 (q, 39 Hz), 122.9 (q, *J* = 273 Hz), 122.6 (q, *J* = 273 Hz), 121.9 (q, *J* = 31 Hz), 120.3, 117.3 (q, *J* = 6 Hz), 66.3, 66.2, 34.5, 29.68 (3C), 29.63, 29.61, 29.58, 29.51, 29.3 (2C), 29.2, 28.9, 25.9, 25.0. HRMS (ESI) *m/z* $[M+H]^+$ calcd for $C_{31}H_{42}F_6NO_4$, 618.3013; found, 618.3009.

General procedure B: Benzyl Ester deprotection

To a solution of the benzyl ester (0.5 mmol) in anhydrous tetrahydrofuran (7 mL) was added a catalytic amount of palladium/charcoal. The reaction mixture was placed under a hydrogen atmosphere and left to stir at room temperature for 18 h. The mixture was filtered through

celite and the celite was rinsed with acetone. The solution was then concentrated under reduced pressure and the residue was purified by DCVC using gradient elutions of dichloromethane/ethyl acetate (100:0 to 60:40).

16-(((3-trifluoromethyl-4-(chloro)phenyl)carbamoyl)oxy)hexadecanoic acid (C1).

White solid, 75% yield. Mp 65-66 °C. ^{1}H NMR (500 MHz, acteone-d_6): 9.10 (s, 1H), 8.13 (d, *J* = 2.5 Hz, 1H), 7.82 (dd, *J* = 9.0, 2.5 Hz, 1H), 7.59 (d, *J* = 8.5 Hz, 1H), 4.17 (t, *J* = 6.5 Hz, 2H), 2.30 (d, *J* = 7.5 Hz, 2H), 1.67 (pent, *J* = 6.5 Hz, 2H), 1.60 (pent, *J* = 7.0 Hz, 2H), 1.43 – 1.20 (m, 22H). ^{13}C NMR (125 MHz, acetone-d_6): 173.73, 153.58, 139.01, 132.00, 127.75 (q, *J* = 31 Hz), 124.09, 122.90 (q, *J* = 247 Hz), 122.63, 116.95, 65.00, 33.29, 29.47, 29.46, 29.45, 29.44, 29.38, 29.34, 29.18, 28.74, 26.65, 24.77. HRMS (ESI) *m/z* $[M+H]^+$ calcd for $C_{24}H_{36}ClF_3NO_4$, 494.2279; found, 494.2270.

16-(((3-chloro-4-(trifluoromethyl)phenyl)carbamoyl)oxy)hexadecanoic acid (C2).

White solid, 85% yield. Mp 95-96 °C. ^{1}H NMR (500 MHz, DMSO-d_6): δ 10.23 (s, 1H), 7.81 (s, 1H), 7.75 (d, *J* = 9.0 Hz, 1H), 7.55 (d, *J* = 9 Hz, 1H), 4.11 (t, *J* = 7.0 Hz, 2H), 2.16 (t, *J* = 7.5 Hz, 2H), 1.61 (p, *J* = 7.0 Hz, 2H), 1.46 (p, *J* = 7.0 Hz, 2H), 1.34-1.22 (m, 22H). ^{13}C NMR (125 MHz, DMSO-d_6): δ 175.0, 153.8, 144.6, 131.7, 129.1, 123.5 (q, *J* = 273 Hz), 120.2 (q, *J* = 31 Hz), 119.9, 116.5, 65.3, 34.1, 29.49, 29.47, 29.45, 29.44, 29.38, 29.36, 29.35, 29.19, 29.04, 29.00, 28.8, 25.7, 25.0. HRMS (ESI) *m/z* $[M+H]^+$ calcd for $C_{24}H_{36}ClF_3NO_4$, 494.2279; found, 494.2275.

16-(((3-chloro-5-(trifluoromethyl)phenyl)carbamoyl)oxy)hexadecanoic acid (C3).

White solid, 65% yield. Mp 69-70 °C. ^{1}H NMR (500 MHz, DMSO-d_6): δ 10.17 (s, 1H), 7.80 (s, 2H), 7.43 (s, 1H), 4.11 (t, *J* = 7.0 Hz, 2H), 1.62 (p, *J* = 7.0 Hz, 2H), 1.46 (p, *J* = 7.0 Hz, 2H), 1.35-1.22 (m, 22H). ^{13}C NMR (125 MHz, DMSO-d_6): δ 174.9, 153.9, 142.1, 134.8, 131.6 (q, *J* = 31 Hz), 123.8 (q, *J* = 273 Hz), 121.4, 118.8, 113.2, 65.3, 34.1, 29.49, 29.47, 29.45, 29.44, 29.37 (2C), 29.35, 29.19, 29.04, 29.00 28.8, 25.7, 25.0. HRMS (ESI) *m/z* $[M+H]^+$ calcd for $C_{24}H_{36}ClF_3NO_4$, 494.2279; found, 494.2269.

16-(((4-((trifluoromethyl)sulfonyl)phenyl)carbamoyl)oxy)hexadecanoic acid (C4).

White solid, 71% yield. Mp 110-112 °C. ^{1}H NMR (500 MHz, DMSO-d_6): δ 10.52 (s, 1H), 8.04-8.02 (m, 2H), 7.87-7.85 (m, 2H), 4.16 (t, *J* = 6.5 Hz, 2H), 2.17 (t, *J* = 7.5 Hz, 2H), 1.62 (p, *J* = 7.0 Hz, 2H), 1.47 (p, *J* = 7.0 Hz, 2H), 1.35-1.22 (m, 22H). ^{13}C NMR (125 MHz, DMSO-d_6): δ 175.0,

153.7, 148.3, 132.9 (2C), 121.3, 119.0 (2C), 118.7, 65.5, 34.1, 29.48, 29.47, 29.46, 29.43, 29.39, 29.38, 29.35, 29.18, 29.06, 28.99, 28.7, 25.7, 24.9. HRMS (ESI) *m/z* $[M+H]^+$ calcd for $C_{24}H_{37}F_3NO_6S$, 524.2288; found, 524.2282.

16-(((3-chloro-5-(pentafluoro-λ^6-sulfaneyl)phenyl)carbamoyl)oxy)hexadecanoic acid (C5).

White solid, 40% yield. Mp 91-92 °C. ^{1}H NMR (500 MHz, DMSO-*d*$_6$): δ 10.23 (s, 1H), 8.03 (s, 1H), 7.78 (s, 1H), 7.62-7.61 (m, 1H), 4.10 (t, *J* = 7.0 Hz, 2H), 2.16 (t, *J* = 7.5 Hz, 2H), 1.61 (p, *J* = 7.0 Hz, 2H), 1.47 (p, *J* = 7.0 Hz, 2H), 1.33-1.21 (m, 22H). ^{13}C NMR (125 MHz, DMSO-*d*$_6$): δ 174.9, 154.1 (q, *J* = 19 Hz), 153.9, 141.8, 134.3, 121.3, 119.4, 114.1, 65.4, 34.1, 29.49, 29.47, 29.45, 29.44, 29.364 (2C), 29.357, 29.19, 29.03, 29.00, 28.7, 25.7, 25.0. HRMS (ESI) *m/z* $[M+H]^+$ calcd for $C_{23}H_{36}ClF_5NO_4S$, 552.1968; found, 552.1967.

16-(((3,4-bis(trifluoromethyl)phenyl)carbamoyl)oxy)hexadecanoic acid (C6).

White solid, 61% yield. Mp 68-69 °C. ^{1}H NMR (500 MHz, DMSO-*d*$_6$): δ 10.39 (s, 1H), 8.14 (s, 1H), 7.95 (d, *J* = 8.5 Hz, 1H), 7.90 (d, *J* = 9.0 Hz, 1H), 4.12 (t, *J* = 7.0 Hz, 2H), 2.16 (t, *J* = 7.0 Hz, 2H), 1.61 (p, *J* = 7.0 Hz, 2H), 1.46 (p, *J* = 7.5 Hz, 2H), 1.34-1.21 (m, 22H). ^{13}C NMR (125 MHz, DMSO-*d*$_6$): δ 174.5, 153.4, 143.6, 129.6 (q, *J* = 6 Hz), 127.0 (q, *J* = 31 Hz), 123.1 (q, *J* = 273 Hz), 122.7 (q, *J* = 273 Hz), 120.6, 118.8 (q, *J* = 31 Hz), 116.6 (q, *J* = 6 Hz), 64.9, 39.0, 29.02, 29.00, 28.99, 28.98, 28.91 (2C), 28.89, 28.73, 28.59, 28.53, 28.29, 25.3, 24.5. HRMS (ESI) *m/z* $[M+H]^+$ calcd for $C_{25}H_{36}F_6NO_4$, 528.2543; found, 528.2544.

Synthesis of A3

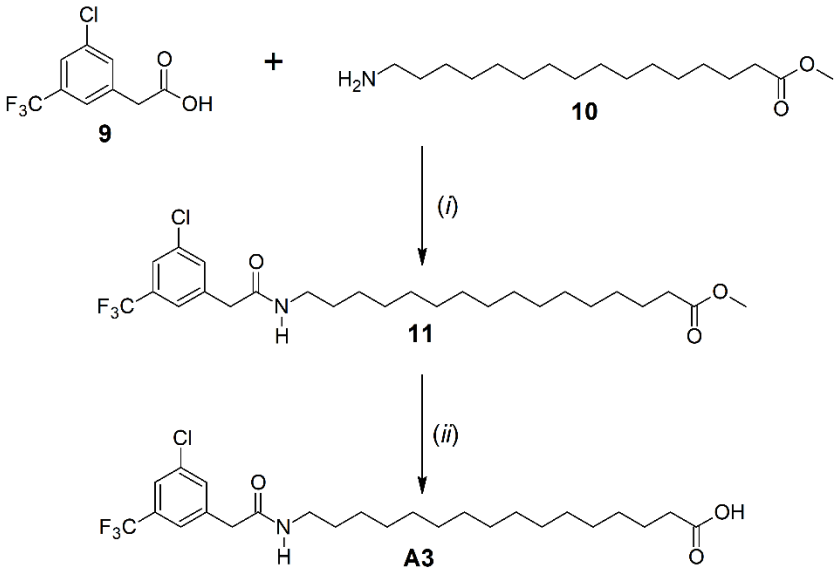

Scheme S1: - Synthesis of aryl-amide **A3**. Reagents and conditions: (i) anhydrous dichloromethane, oxalyl chloride, rt, 19 h; (iii) ethanol, 1.5M NaOH, 40°C, 4 h.

Methyl 16-(2-(3-chloro-5-(trifluoromethyl)phenyl)acetamido)hexadecanoate (11).

Phenyl acetic acid **9** (0.200 g, 0.84 mmol) was dissolved in anhydrous dichloromethane (7 mL) under a nitrogen atmosphere. Oxalyl chloride (0.117 g, 0.92 mmol) was added dropwise and the resulting solution was stirred for 1 h. **10** (0.239 g, 0.84 mmol) was then added and the reaction stirred for 18 h. The reaction was diluted with water (50 mL) and extracted with dichloromethane (3 x 70 mL). The combined extracts were dried over Mg_2SO_4 and concentrated under reduced pressure. The residue was purified on silica gel by stepwise gradient elution with dichloromethane/ethyl acetate (100:0 to 70:30), yielding **11** (0.089 g, 21%) was a white solid. Mp 87-88 ^{o}C. ^{1}H NMR (500 MHz, CDCl3): δ 7.53 (s, 1H), 7.49 (s, 1H), 7.43 (s, 1H), 5.43 (s, 1H), 3.66 (s, 3H), 3.55 (s, 2H), 3.26-3.22 (q, *J* = 7 Hz, 2H), 2.30 (t, *J* = 7.5 Hz, 2H), 1.60 (p, *J* = 7.0 Hz, 2H), 1.49-1.45 (p, *J* = 7 Hz, 2H), 1.28-1.24 (m, 22H). ^{13}C NMR (125 Hz, $CDCl_3$): δ 173.95, 169.24, 134.17, 133.71, 133.70, 131.70, 131.19, 128.60 (q, *J* = 31 Hz), 128.42 (q, *J* = 5 Hz), 122.66 (q, *J* = 272 Hz), 51.57, 42.73, 34.39, 29.59 (2C), 29.58, 29.55, 29.51,

29.47, 29.42, 29.24, 29.21, 29.13. HRMS (ESI) *m/z* $[M+H]^+$ calcd for $C_{26}H_{40}ClF_3NO_3$, 506.2623; found, 506.2619.

16-(2-(3-chloro-5-(trifluoromethyl)phenyl)acetamido)hexadecanoic acid (A3).

1.5M NaOH (5 mL) was added to a solution of ester **11** (0.070 g, 0.14 mmol) in ethanol (15 mL), and the solution was stirred at 40 °C for 3 h. The mixture was acidified to pH 2 using 1M HCl. The resulting suspension was filtered and the solid washed with H_2O (5 mL) and ethanol (3 mL). The solid was dried under reduced pressure, yielding **A3** (0.064 g, 94%) as a white solid. Mp 90-91 °C. ^{1}H NMR (500 MHz, acetone-d_6): δ 7.68 (s, 1H), 7.64 (s, 1H), 7.63 (s, 1H), 7.37 (s, 1H), 3.65 (s, 2H), 3.20 (q, *J* = 5.5 Hz, 2H), 2.27 (t, *J* = 7.0 Hz, 2H), 1.60 (p, *J* = 7.0 Hz, 2H), 1.47 (p, *J* = 7.0 Hz, 2H), 1.40-1.25 (m, 22H). ^{13}C NMR (125 MHz, DMSO-d_6): 174.95, 169.40, 137.19, 135.21, 131.81, 129.08, 128.64 (q, *J* = 5 Hz), 126.72 (q, *J* = 30 Hz), 123.34 (q, *J* = 271 Hz), 41.61, 39.01, 29.47 (3C), 29.43, 29.42, 29.41, 29.40, 29.35, 29.19, 29.14, 29.00. HRMS (ESI) *m/z* $[M+H]^+$ calcd for $C_{25}H_{38}ClF_3NO_3$, 492.2487; found, 492.2481.

4. Experimental Procedures- Biology

Cell culture and cell-based assays.

Human MDA-MB-231 breast cancer cells were obtained from ATCC (Manassas, VA, USA) and were grown at 37°C in a humidified atmosphere of 5% CO_2 in air in DMEM supplemented with 10% fetal bovine serum (Thermo Fischer Scientific) and 1% penicillin/streptomycin (Invitrogen). Confluent cells (80-90%) were harvested using Trypsin/EDTA after washing with PBS. Cells were treated with various concentrations of the test compounds in DMSO (final concentration 0.1%); control cells were treated with DMSO alone.

ATP assay: MDA-MB-231 cells were seeded in triplicate in 96-well plates (7.5×10^4 cells/well) and allowed to adhere overnight. After serum starvation for 24 h cells were treated with various concentrations of the test compounds for 48 h; control cells received serum-free DMEM. Cells were incubated with CellTiter-Glo in serum-free medium (RT, 10 min) and luminescence was determined (CellTiter-Glo® luminescent cell viability assay, Promega; Annandale, NSW, Australia).

JC-1 assay: MDA-MB-231 cells were seeded in triplicate in 96-well plates (1×10^4 cells/well) and allowed to adhere overnight. After serum starvation for 24 h cells were treated with various concentrations of the test compounds for 1 h; control cells received serum-free DMEM. Cells were incubated with JC-1 in serum-free medium (37°C, 20 min) and the JC-1 red:green ratio was estimated (JC-1 Mitochondrial Membrane Potential Assay Kit; Cayman Chemical, Ann Arbor, MI).

LDH assay: MDA-MB-231 cells well seeded in triplicate in 96 well plates (1.0x104 cells per well). Media was removed and cells were treated with test compounds (20 µM) or vehicle control and incubated for 48 hours. For positive control cells were treated with), 0.2% (v/v) Triton X-100 (positive control) Well media was homogenised gently, sampled, diluted in LDH storage buffer and stored at -20° C. Samples were thawed prior to analysis and extracellular LDH activity was determined using the LDH-Glo™ Cytotoxicity Assay (Promega, Alexandria, NSW, Australia) according to the manufacturer's instructions.

Mitochondrial function: Mitochondrial function was measured by determining the oxygen consumption rate (OCR) of cells with a Seahorse XF24 extracellular flux analyser (Seahorse

Bioscience, MA, USA) according to the manufacturer's protocols. MDA-MB-231 cells were seeded in 24-well XF cell culture microplates (2.5×10^4 cells per well) and allowed to adhere overnight (37 °C, 5% CO2). After serum starvation for 24 h, culture medium was replaced with buffered XF Base Medium supplemented with 2 mM L-glutamine, 10 mM glucose and 2 mM sodium pyruvate at pH 7.4. The cells were incubated at 37 °C without CO_2 for an hour, and then the OCR was measured utilizing an XF Cell Mito Stress Test Kit (Seahorse Bioscience, MA, USA). Oligomycin (final concentration 1 µM), carbonylcyanide m-chlorophenylhydrazone (FCCP-final concentration 0.5 µM, or test compounds - final concentrations 20 µM), and rotenone/antimycin A (final concentrations 0.5 µM each) were added to the sensor cartridge, and the OCR was measured using a modified cycling program.

Data Analysis: Biological data were processed and statistically analysed in GraphPad Prism 8.3.0 for Windows (GraphPad Software, San Diego, California USA, www.graphpad.com) through t-tests using the Holm-Sidak method, with alpha = 0.05. Each row was analysed individually, without assuming a consistent SD. All data expressed throughout as means ± SEM. All experiments were replicated as indicated.

5. Experimental Procedures- Tethered bilayer lipid membranes

Lipid bilayers were anchored to a gold electrode according to "T10" architecture. This consists of 10% benzyl-disulfide (tetra-ethyleneglycol) n=2 C20-phytanyl "tethering" molecules interspersed with 90% benzyl-disulfide-tetra-ethyleneglycol-OH "spacer" molecules. Spacer and tether molecules are all coordinated onto a 2.1 mm^2 gold tethering electrode. To these first layer chemistries were added a second layer of mobile phase lipid molecules of 3 mM 1,2-dioleoyl-sn-glycero-3-phosphocholine (DOPC) (Avanti Polar Lipids Inc., Alabaster, USA) which was left to incubate with the tethering molecules for 2 min before a rapid exchange of 3 x 400 µL 5 mM Me_4NPF_6/HEPES buffer (adjusted to pH 7.5 with NaOH) induced the formation of a completed tBLM.

Swept frequency electrical impedance spectroscopy ranging from 0.1 Hz to 2000 Hz was applied at 25 mV peak-to-peak, using a Tethapod™ electrical impedance spectrometer (SDx Tethered Membranes Pty Ltd). Impedance and phase profiles were fitted to an equivalent circuit consisting of a constant phase element, representing the tethering gold electrode and reservoir region, in series with a resistor, to represent the impedance of the surrounding electrolyte solution, and a resistor/capacitor representing the lipid bilayer (as described previously)[3]. Data fitting utilized a proprietary adaptation of a Levenberg–Marquardt fitting routine incorporated into the TethaQuick™ software (SDx Tethered Membranes Pty Ltd).

6. Experimental Procedures- NMR Studies

Bromide binding studies

^{1}H NMR titration of **C3** benzyl ester and **U3** methyl ester with TBABr in $CDCl_3$ was performed on a Bruker Avance III 500 MHz at 298 K, using 600 µL of 1 mM host solution of $CDCl_3$. Stock solutions of TBABr (100 mM) used as the titrant contained 1 mM of the host to prevent host dilution throughout the titration.

Concentration-dependent ^{1}H NMR studies

$CDCl_3$ was deacidified by K_2CO_3 treatment followed by filtration prior to use. A few milligrams of compound **C3** was weighed in a vial and treated with 1.0 equivalent of tetrabutylammonium hydroxide (TBAOH, 40% in H_2O). ~0.5 mL of $CDCl_3$ was added and the mixture was sonicated to assist the mixing. The mixture was evaporated using a stream of N_2 gas. The $CDCl_3$ addition and evaporation were repeated twice to ensure complete removal of water. $CDCl_3$ was then added to the residue to a prepare a 5 mM **C3**-TBAOH solution. The solution was diluted to various concentrations in $CDCl_3$ and subject to ^{1}H NMR measurements on a Bruker Ascend 700 NMR spectrometer equipped with a TCI cryoprobe.

Diffusion NMR studies

Pulse field gradient diffusion NMR experiments were performed on a Bruker Advance III 600 MHz Cryo NMR at 298 K with uncalibrated gradient strengths. The data were analysed using Bruker TopSpin 4.0.9. To obtain the absolute diffusion coefficients, the diffusion coefficient of $CHCl_3$ in $CDCl_3$ was measured and compared with a literature value.[1] The ratio between the literature and experimental values of diffusion coefficient of $CHCl_3$ was used to calibrate the data.

5. Computational Methodology

Density Functional Theory Calculations

Density functional theory (DFT) calculations were used to examine the complexation of carboxylates to compounds in Table 1. As in our previous work, model compounds were constructed by truncating the tail of compounds in Table 1 to a propyl moiety.[2] Additionally, propanoate was used as a substitute for a longer chain fatty acid. All calculations were performed with Gaussian16 Revision C.01.[3] Geometry optimizations were conducted at the M06-2X-D3(0)/6-311+G(d) level of theory followed by single point calculations at the DSD-PBEP86/aug-cc-pVTZ level of theory.[4–12] The use of double hybrid DFT for single points in conjunction with a large diffuse basis set is expected to provide accurate gas phase reaction energetics for the anionic species studied herein.[13] Frequency calculations were conducted at each optimized geometry to ensure a minimum on the potential energy surface had been obtained. If compounds were not symmetric with respect to rotation of the aryl system, the rotamer with the lowest electronic energy in each respective solvent was selected. Gas phase free energies were obtained by inclusion of zero-point vibrational energy, thermal corrections and entropies calculated from the frequencies of the M06-2X-D3(0)/6-311+G(d) optimised geometry. Solution free energies in water and n-pentadecane were obtained using the SMD solvation model, following the recommendations of Ho and Coote.[14] Cumulatively, this resulted in data at the DSD-PBEP86/aug-cc-pVTZ//M06-2X-D3(0)/6-311+G(d) in the gas phase and in two solvents for the carbamate and aryl-urea series. Gaussian archive entries for each calculation and coordinates of all stationary points are available on github at https://github.com/hmacdope/carbamide_uncouplers. Natural Population Analysis calculations[15] were conducted on the gas phase optimised geometries at the DSD-PBEP86/aug-cc-pVTZ level of theory.

Molecular Dynamics Simulations

Critical to uncoupling activity or lack thereof are dynamics of the uncoupler in a lipid bilayer environment. To examine this, we conducted molecular dynamics simulations of **C3** in various protonation states in a 128-lipid united-atom DOPC bilayer. Both protonated (carboxylic acid) and deprotonated (carboxylate) protomers of the fatty acid tail were examined, denoted as

C3 and **C3-D**, where the suffix **-D** indicates the deprotonated (carboxylate) form. GROMOS-54A7 parameters for **C3** and **C3-D** were obtained from the Automated Topology Builder at the QM1 parameterisation level.[16] Parameters for DOPC were those of Poger *et al*.[17,18] The 128 lipid DOPC bilayer with the lipids oriented in the x-y plane was obtained pre-equilibrated from the ATB, extended in the z dimension, re-solvated and re-equilibrated. 10 molecules of the target compound (**C3** or **C3-D**) were placed randomly in the water layer above the upper leaflet. Each system was then neutralised and 100 mM of NaCl was added. This process was conducted 3 times to yield 3 replicates of each system. Each replicate was simulated for 1 µs yielding 6 µs of simulation across the two systems.

In addition to systems containing only a single target compound, the behaviour of a system with a mix of target compound protonation states were investigated. This involved addition of 5 molecules of carboxylic acids **C3** to the **C3-D** systems respectively, following 1 µs of simulation. As above, three replicates were created for each system and simulated for 1 µs each, yielding an additional 6 µs of simulation. Simulation protocol was identical to that of our previous work,[2] with the exception that GROMACS 2019.4 was used instead of GROMACS 2018.[19–22] Analysis was conducted with VMD[23] and Python scripts employing the MDTraj package.[24] Molecular dynamics topologies and run input files used in this work are available on github at https://github.com/hmacdope/carbamide_uncouplers

6. Bibliography

(1) Kato, H.; Saito, T.; Nabeshima, M.; Shimada, K.; Kinugasa, S. Assessment of Diffusion Coefficients of General Solvents by PFG-NMR: Investigation of the Sources Error. *J. Magn. Reson.* **2006**, *180* (2), 266–273.

(2) Rawling, T.; MacDermott-Opeskin, H.; Roseblade, A.; Pazderka, C.; Clarke, C.; Bourget, K.; Wu, X.; Lewis, W.; Noble, B.; Gale, P. A.; et al. Aryl Urea Substituted Fatty Acids: A New Class of Protonophoric Mitochondrial Uncoupler That Utilises a Synthetic Anion Transporter. *Chem. Sci.* **2020**.

(3) Frisch, M. J.; Trucks, G. W.; Schlegel, H. B.; Scuseria, G. E.; Robb, M. a.; Cheeseman, J. R.; Scalmani, G.; Barone, V.; Petersson, G. a.; Nakatsuji, H.; et al. Gaussian 16, Revision C.01. Gaussian Inc 2016.

(4) Zhao, Y.; Truhlar, D. G. The M06 Suite of Density Functionals for Main Group Thermochemistry, Thermochemical Kinetics, Noncovalent Interactions, Excited States, and Transition Elements: Two New Functionals and Systematic Testing of Four M06-Class Functionals and 12 Other Function. *Theor. Chem. Acc.* **2008**, *120* (1–3), 215–241.

(5) Dill, J. D.; Pople, J. A. Self-Consistent Molecular Orbital Methods. XV. Extended Gaussian-Type Basis Sets for Lithium, Beryllium, and Boron. *J. Chem. Phys.* **1975**, *62* (7), 2921–2923.

(6) Clark, T.; Chandrasekhar, J.; Spitznagel, G. W.; Schleyer, P. V. R. Efficient Diffuse Function-augmented Basis Sets for Anion Calculations. III. The 3-21+G Basis Set for First-row Elements, Li–F. *J. Comput. Chem.* **1983**, *4* (3), 294–301.

(7) Frisch, M. J.; Pople, J. A.; Binkley, J. S. Self-Consistent Molecular Orbital Methods 25. Supplementary Functions for Gaussian Basis Sets. *J. Chem. Phys.* **1984**, *80* (7), 3265–3269.

(8) Francl, M. M.; Pietro, W. J.; Hehre, W. J.; Binkley, J. S.; Gordon, M. S.; DeFrees, D. J.; Pople, J. A. Self-Consistent Molecular Orbital Methods. XXIII. A Polarization-Type Basis Set for Second-Row Elements. *J. Chem. Phys.* **1982**, *77* (7), 3654–3665.

(9) Kozuch, S.; Martin, J. M. L. DSD-PBEP86: In Search of the Best Double-Hybrid DFT with Spin-Component Scaled MP2 and Dispersion Corrections. *Phys. Chem. Chem. Phys.* **2011**, *13* (45), 20104–20107.

(10) Dunning, T. H. Gaussian Basis Sets for Use in Correlated Molecular Calculations. I. The Atoms Boron through Neon and Hydrogen. *J. Chem. Phys.* **1989**, *90* (2), 1007–1023.

(11) Woon, D. E.; Dunning, T. H. Gaussian Basis Sets for Use in Correlated Molecular Calculations. III. The Atoms Aluminum through Argon. *J. Chem. Phys.* **1993**, *98*, 1358–1371.

(12) Wilson, A. K.; Woon, D. E.; Peterson, K. A.; Dunning, T. H. Gaussian Basis Sets for Use in Correlated Molecular Calculations. IX. The Atoms Gallium through Krypton. *J. Chem. Phys.* **1999**, *110* (16), 7667–7676.

(13) Goerigk, L.; Mehta, N. A Trip to the Density Functional Theory Zoo: Warnings and Recommendations for the User. *Aust. J. Chem.* **2019**, *72* (8), 563–573.

(14) Ho, J.; Klamt, A.; Coote, M. L. Comment on the Correct Use of Continuum Solvent Models. *J. Phys. Chem. A* **2010**, *114* (51), 13442–13444.

(15) Reed, A. E.; Weinstock, R. B.; Weinhold, F. Natural Population Analysis. *J. Chem. Phys.* **1985**, *83* (2), 735–746.

(16) Malde, A. K.; Zuo, L.; Breeze, M.; Stroet, M.; Poger, D.; Nair, P. C.; Oostenbrink, C.; Mark, A. E. An Automated Force Field Topology Builder (ATB) and Repository: Version 1.0. *J. Chem. Theory Comput.* **2011**, *7* (12), 4026–4037.

(17) Poger, D.; Van Gunsteren, W. F.; Mark, A. E. A New Force Field for Simulating Phosphatidylcholine Bilayers. *J. Comput. Chem.* **2010**, *31* (6), 1117–1125.

(18) Schmid, N.; Eichenberger, A. P.; Choutko, A.; Riniker, S.; Winger, M.; Mark, A. E.; van Gunsteren, W. F. Definition and Testing of the GROMOS Force-Field Versions 54A7 and 54B7. *Eur. Biophys. J.* **2011**, *40* (7), 843–856.

(19) Van Der Spoel, D.; Lindahl, E.; Hess, B.; Groenhof, G.; Mark, A. E.; Berendsen, H. J. C. GROMACS: Fast, Flexible, and Free. *J. Comput. Chem.* **2005**, *26* (16), 1701–1718.

(20) Abraham, M. J.; Murtola, T.; Schulz, R.; Páll, S.; Smith, J. C.; Hess, B.; Lindah, E.

Gromacs: High Performance Molecular Simulations through Multi-Level Parallelism from Laptops to Supercomputers. *SoftwareX* **2015**, *1–2*, 19–25.

(21) Berendsen, H. J. C.; van der Spoel, D.; van Drunen, R. GROMACS: A Message-Passing Parallel Molecular Dynamics Implementation. *Comput. Phys. Commun.* **1995**, *91* (1–3), 43–56.

(22) Páll, S.; Zhmurov, A.; Bauer, P.; Abraham, M.; Lundborg, M.; Gray, A.; Hess, B.; Lindahl, E. Heterogeneous Parallelization and Acceleration of Molecular Dynamics Simulations in GROMACS. *J. Chem. Phys.* **2020**, *153* (13), 134110.

(23) Humphrey, W.; Dalke, A.; Schulten, K. VMD: Visual Molecular Dynamics. *J. Mol. Graph.* **1996**, *14* (1), 33–38.

(24) McGibbon, R. T.; Beauchamp, K. A.; Harrigan, M. P.; Klein, C.; Swails, J. M.; Hernández, C. X.; Schwantes, C. R.; Wang, L. P.; Lane, T. J.; Pande, V. S. MDTraj: A Modern Open Library for the Analysis of Molecular Dynamics Trajectories. *Biophys. J.* **2015**, *109* (8), 1528–1532.

(25) Dyari, H. R. E.; Rawling, T.; Bourget, K.; Murray, M., Synthetic ω-3 Epoxyfatty Acids As Antiproliferative and Pro-apoptotic Agents in Human Breast Cancer Cells. *J. Med. Chem.* **2014**, 57 (17), 7459-7464

7. ^{1}H and ^{13}C NMR spectra

^{1}H NMR spectrum of **3** (500 MHz, $CDCl_3$)

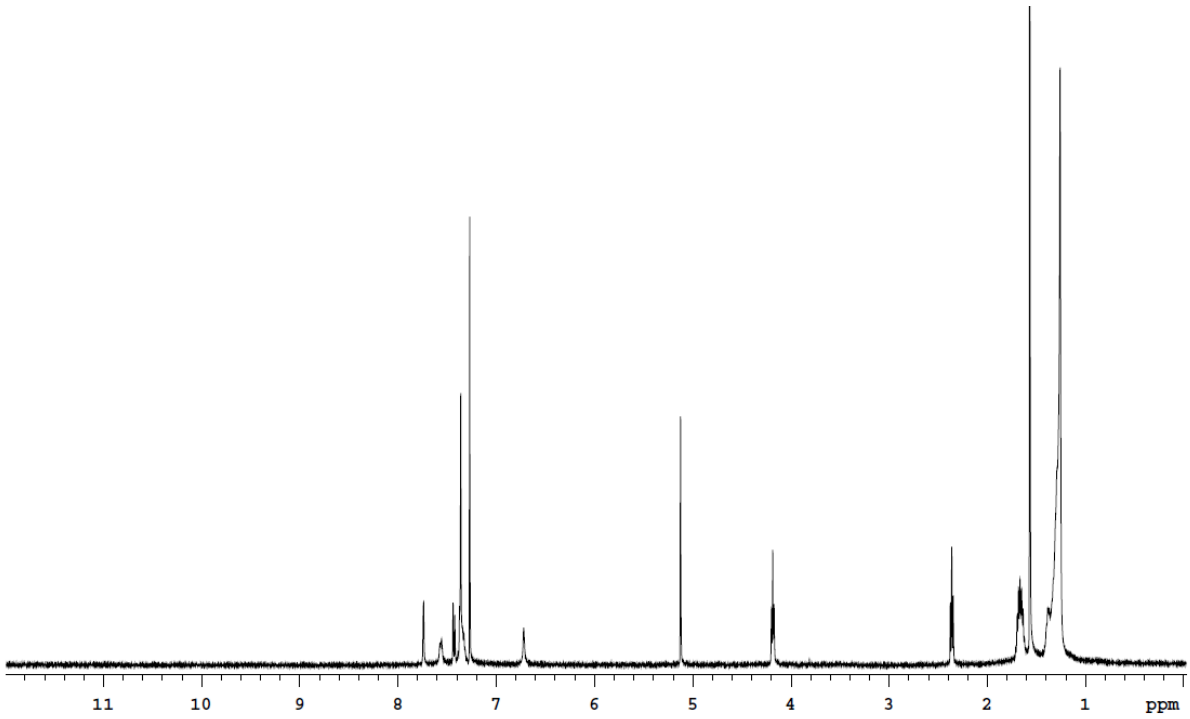

^{13}C NMR spectrum of **3** (125 MHz, $CDCl_3$)

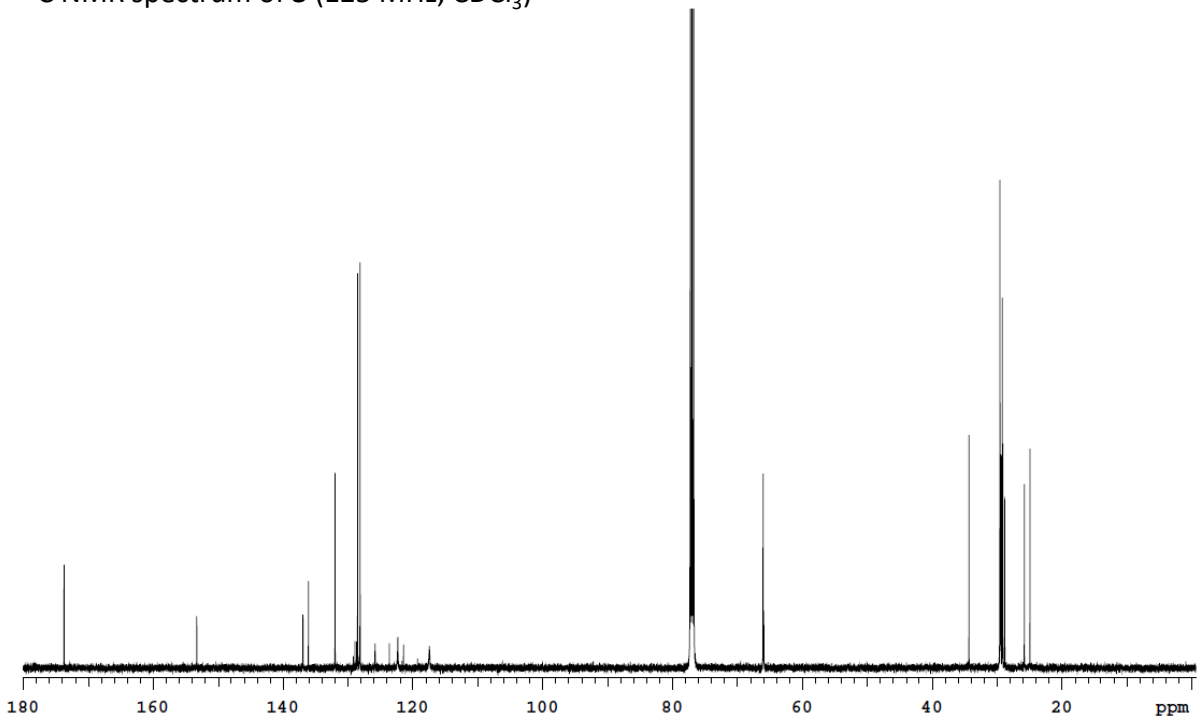

^{1}H NMR spectrum of **4** (500 MHz, $CDCl_3$)

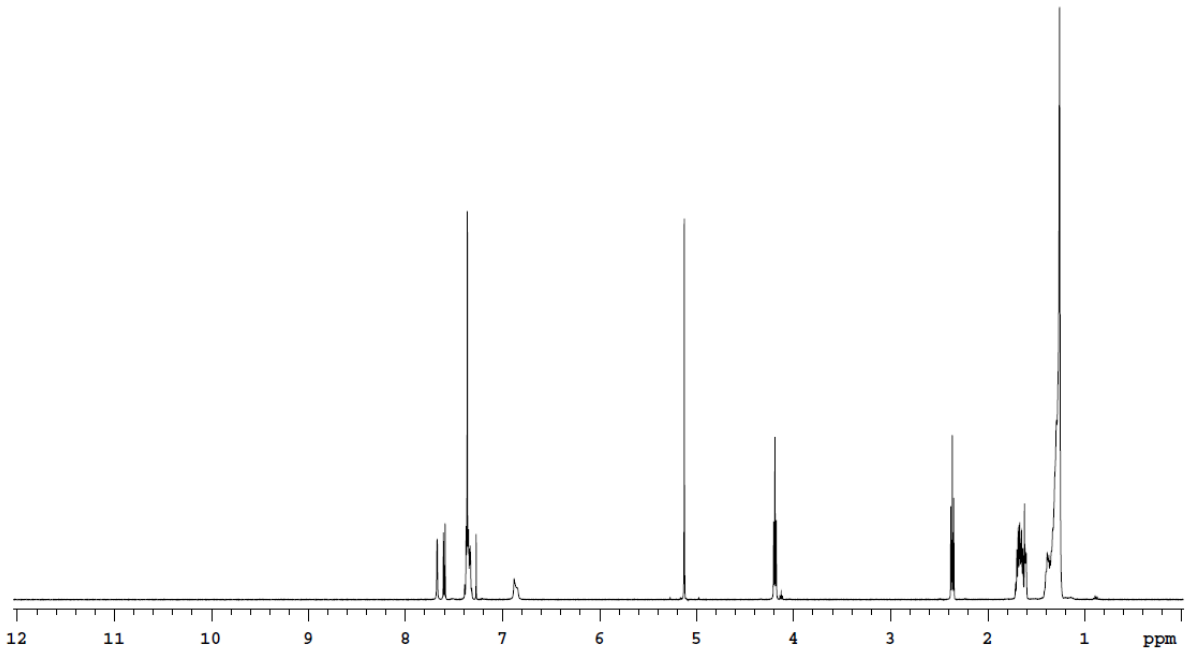

^{13}C NMR spectrum of **4** (125 MHz, $CDCl_3$)

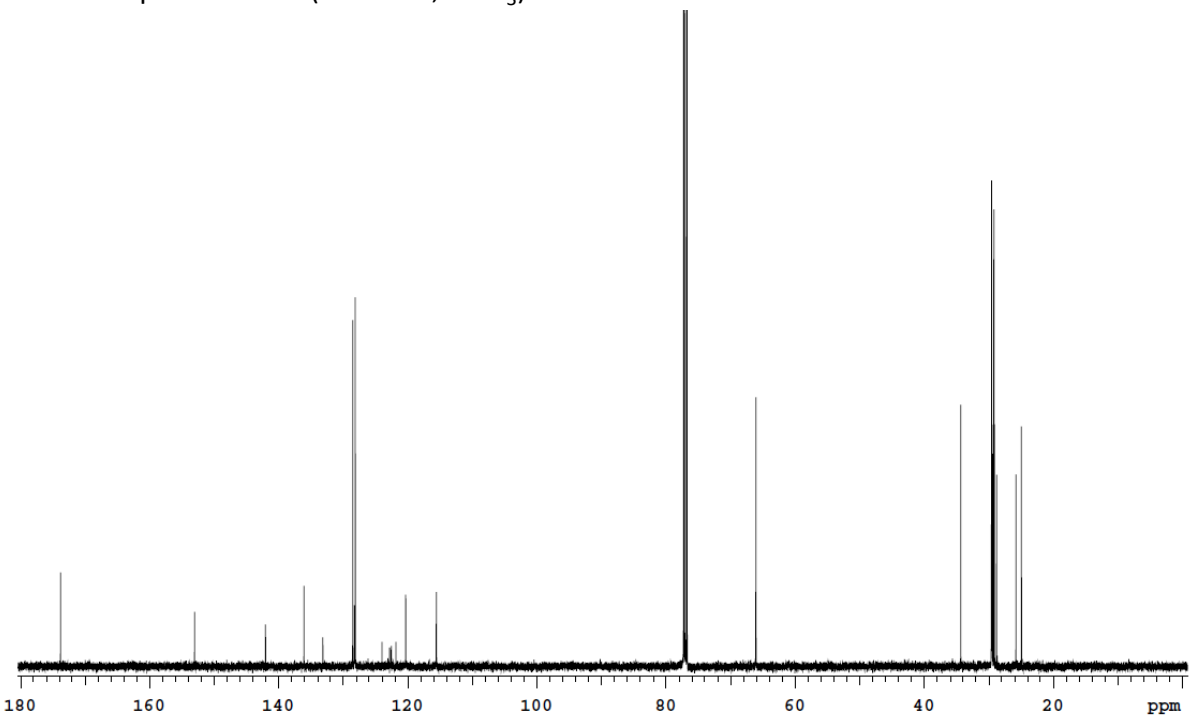

^{1}H NMR spectrum of **5** (500 MHz, $CDCl_3$)

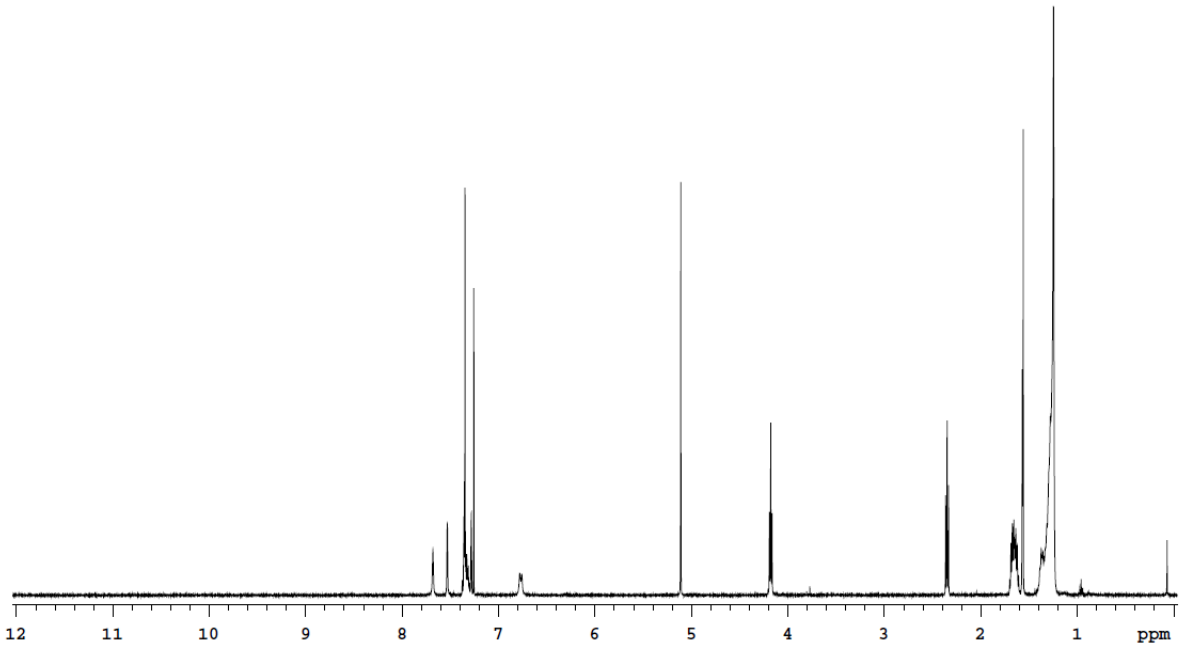

^{13}C NMR spectrum of **5** (125 MHz, $CDCl_3$)

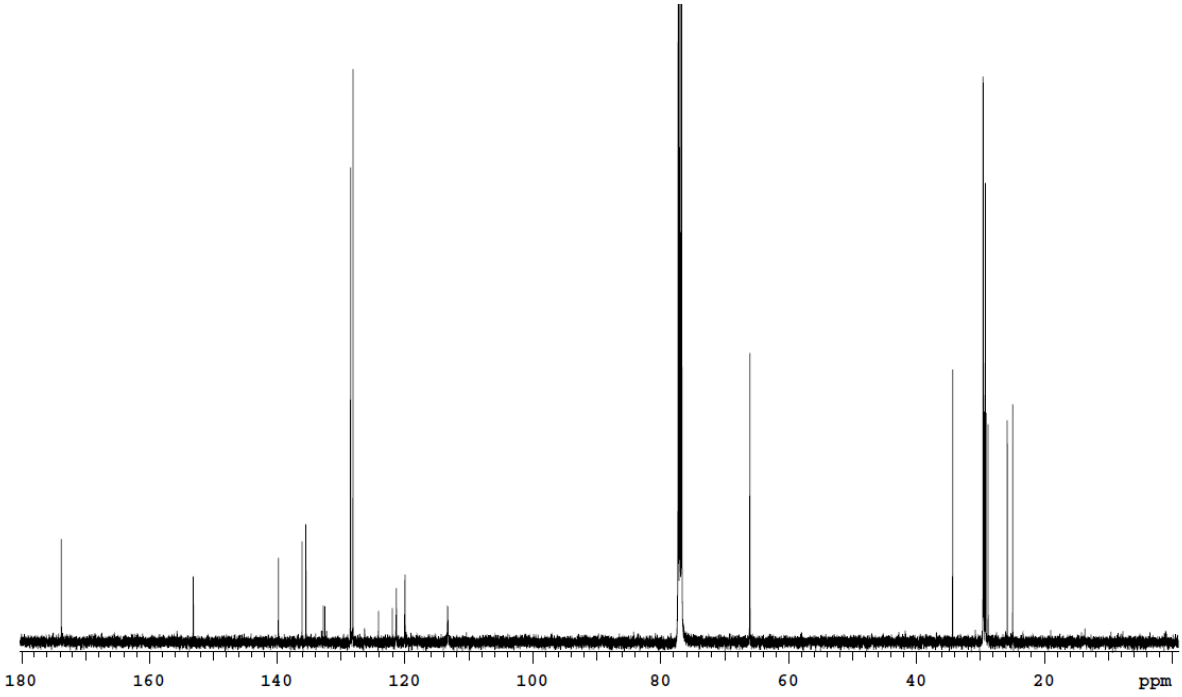

^{1}H NMR spectrum of **6** (500 MHz, $CDCl_3$)

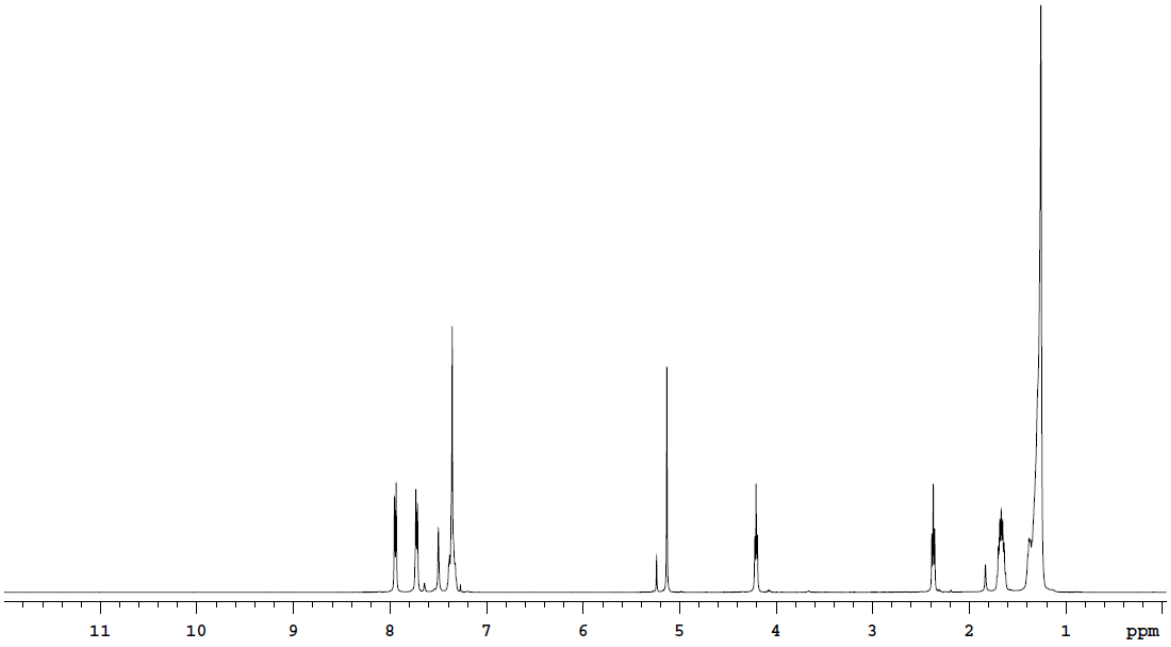

^{13}C NMR spectrum of **6** (125 MHz, $CDCl_3$)

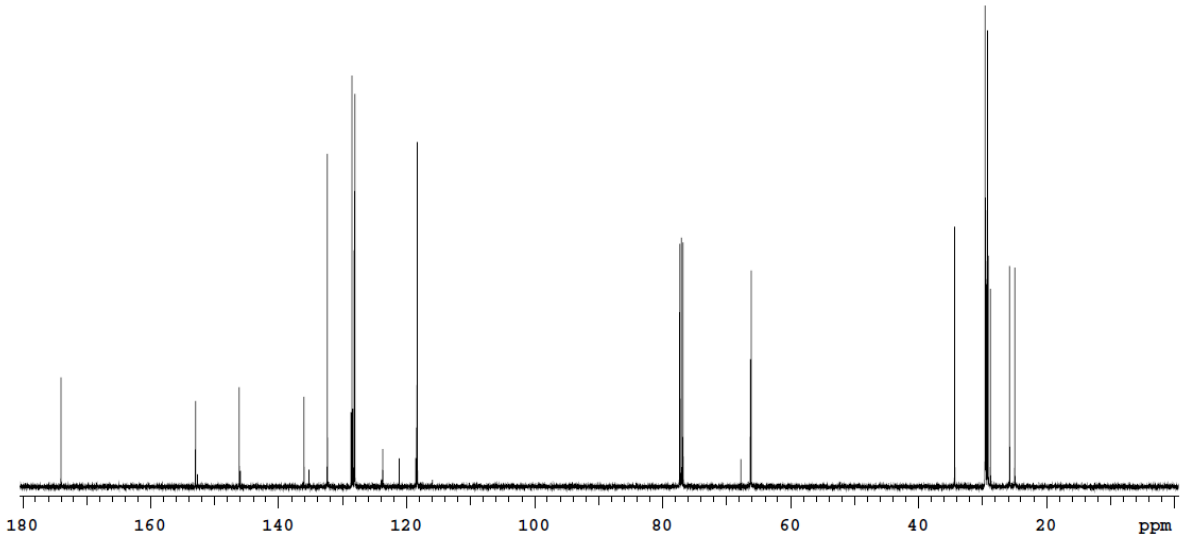

^{1}H NMR spectrum of **7** (500 MHz, $CDCl_3$)

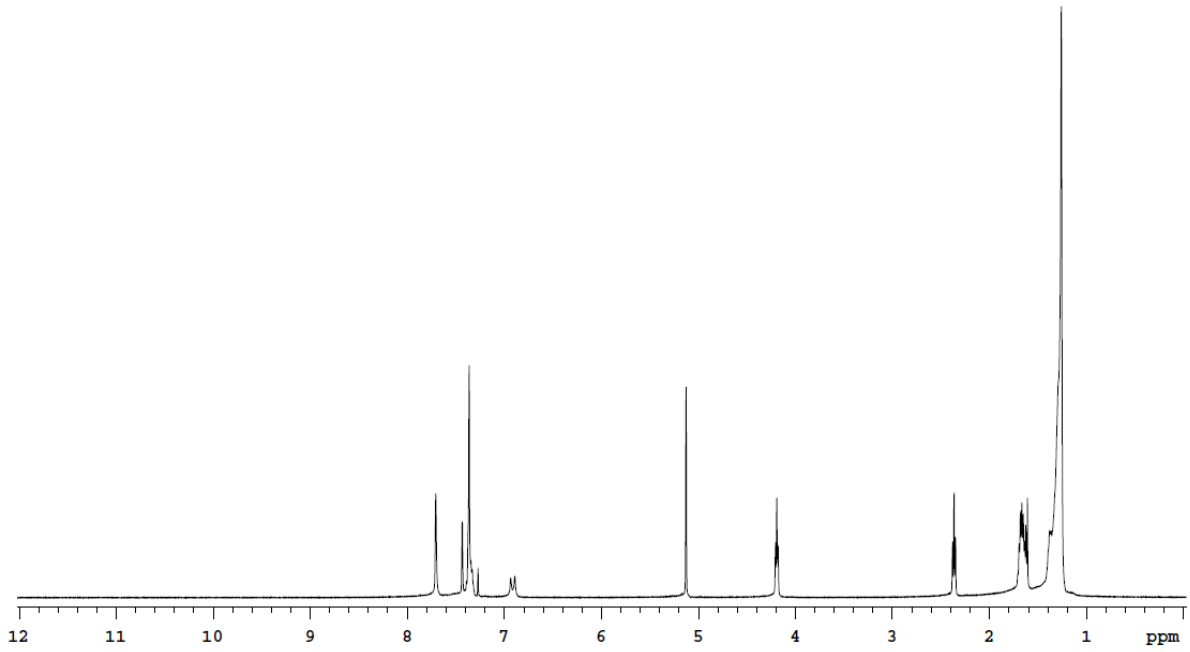

^{13}C NMR spectrum of **7** (125 MHz, $CDCl_3$)

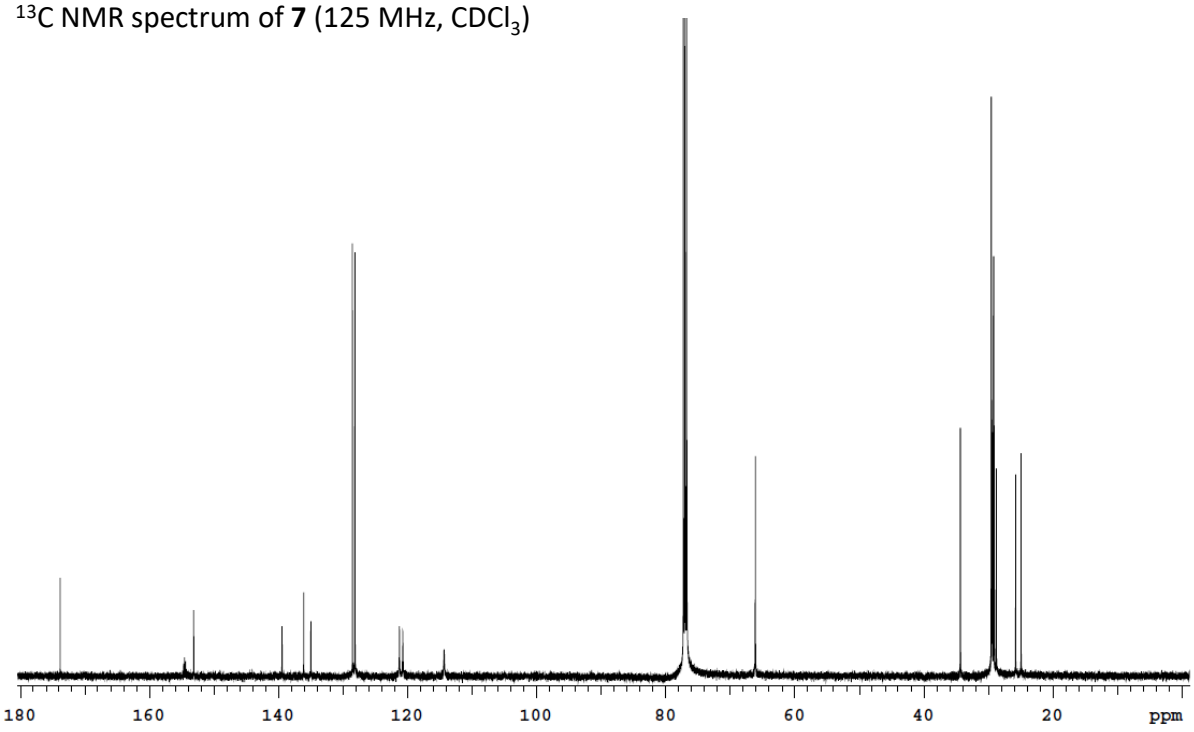

^{1}H NMR spectrum of **8** (500 MHz, $CDCl_3$)

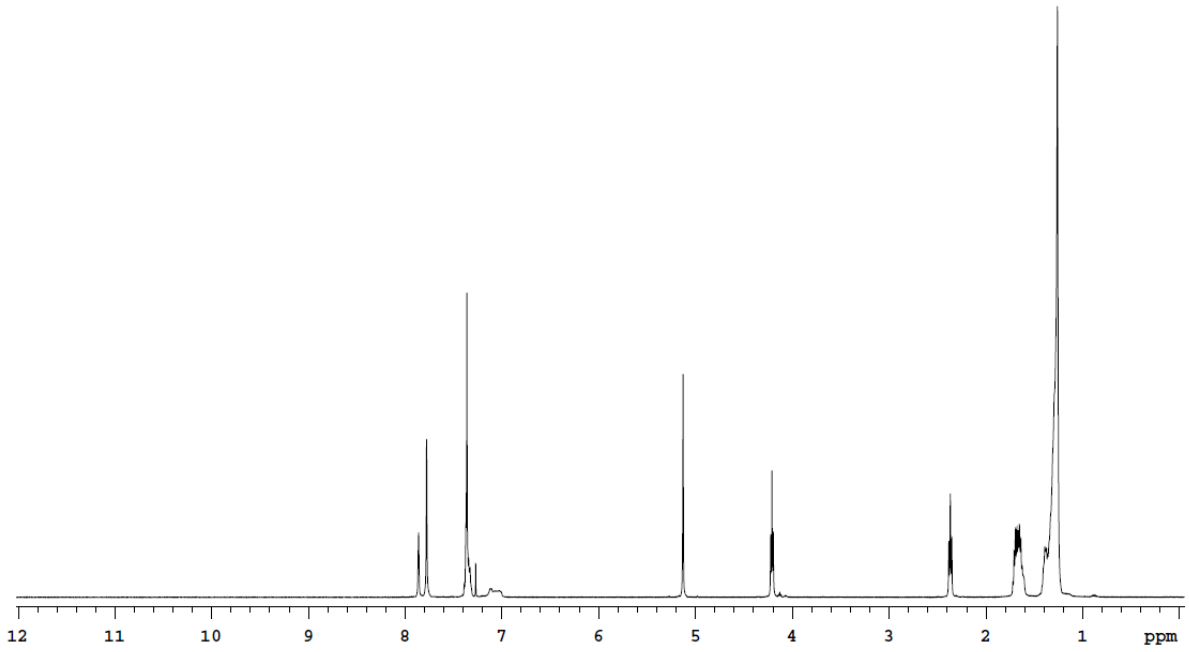

^{13}C NMR spectrum of **8** (125 MHz, $CDCl_3$)

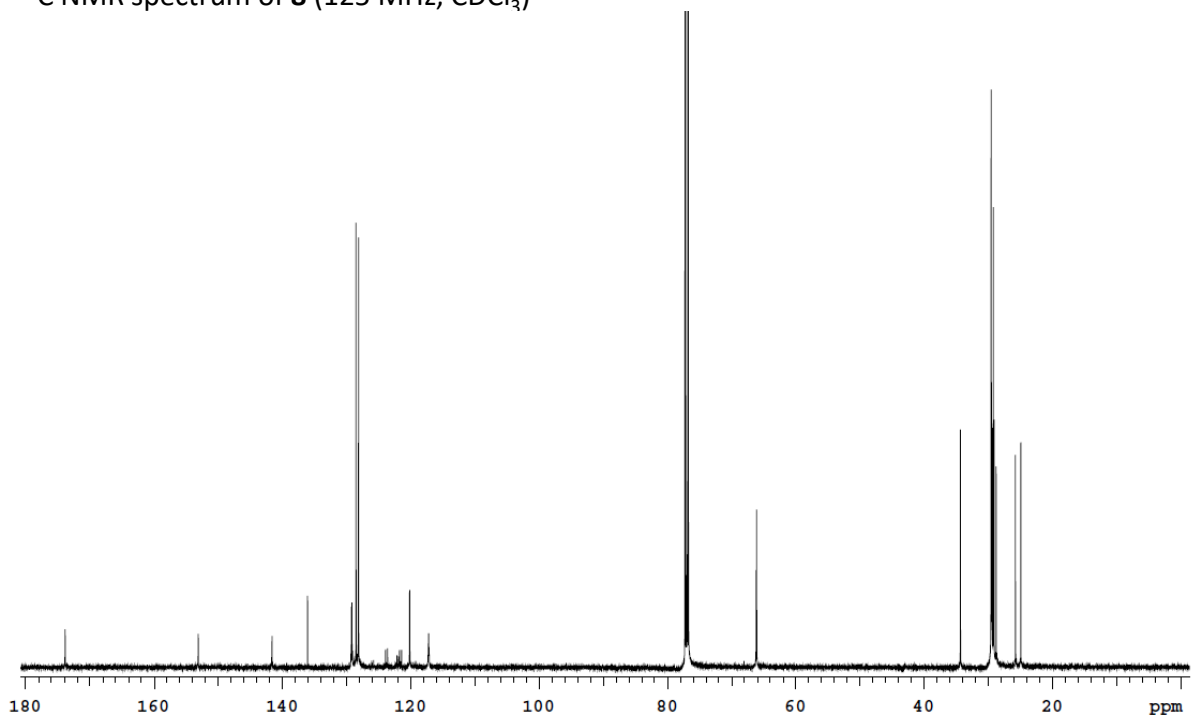

^{1}H NMR spectrum of **C1** (500 MHz, acetone-d_6)

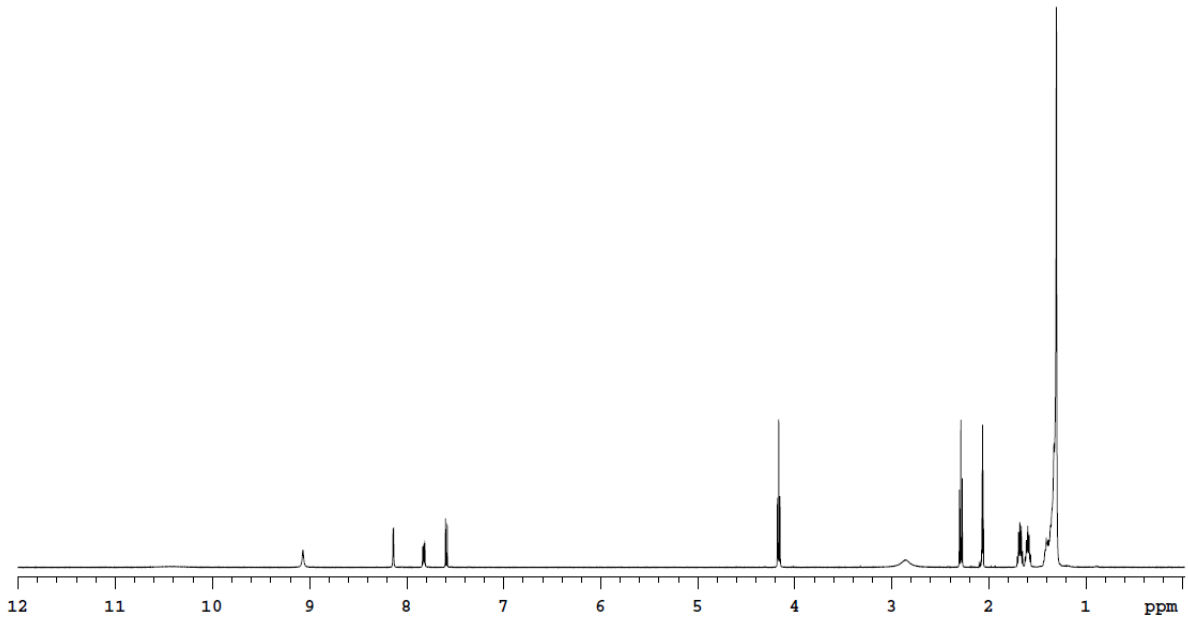

^{13}C NMR spectrum of **C1** (125 MHz, acetone-d_6)

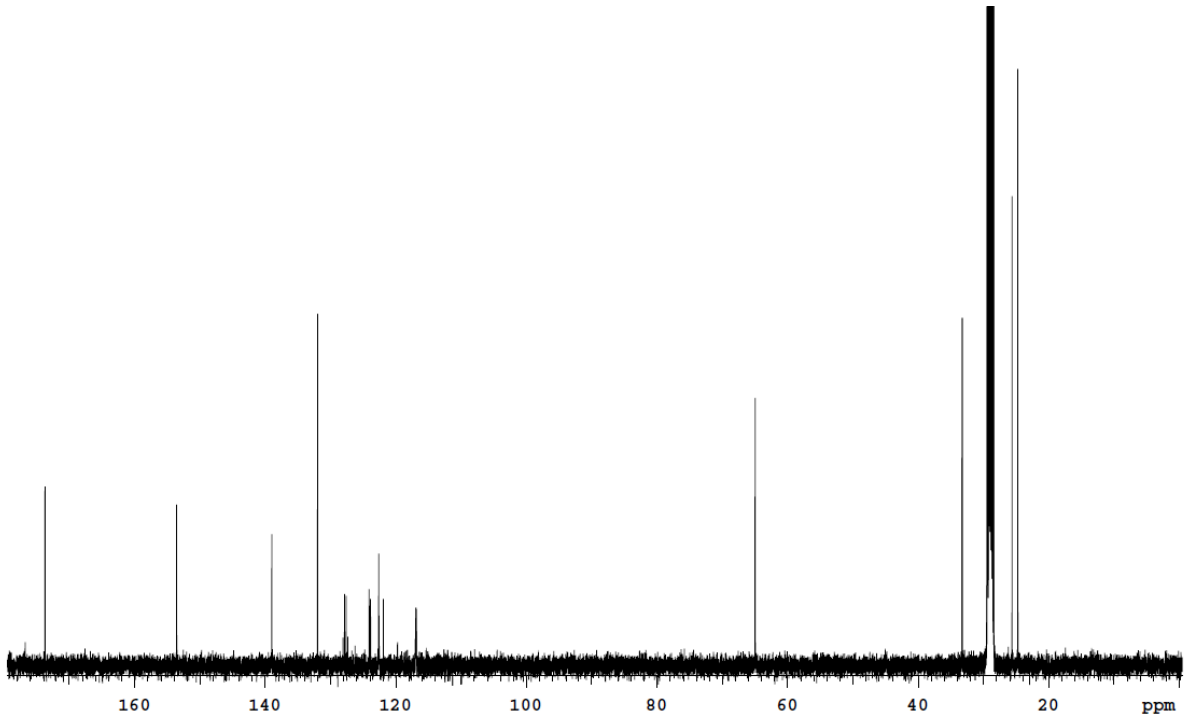

^{1}H NMR spectrum of **C2** (500 MHz, DMSO-d_6)

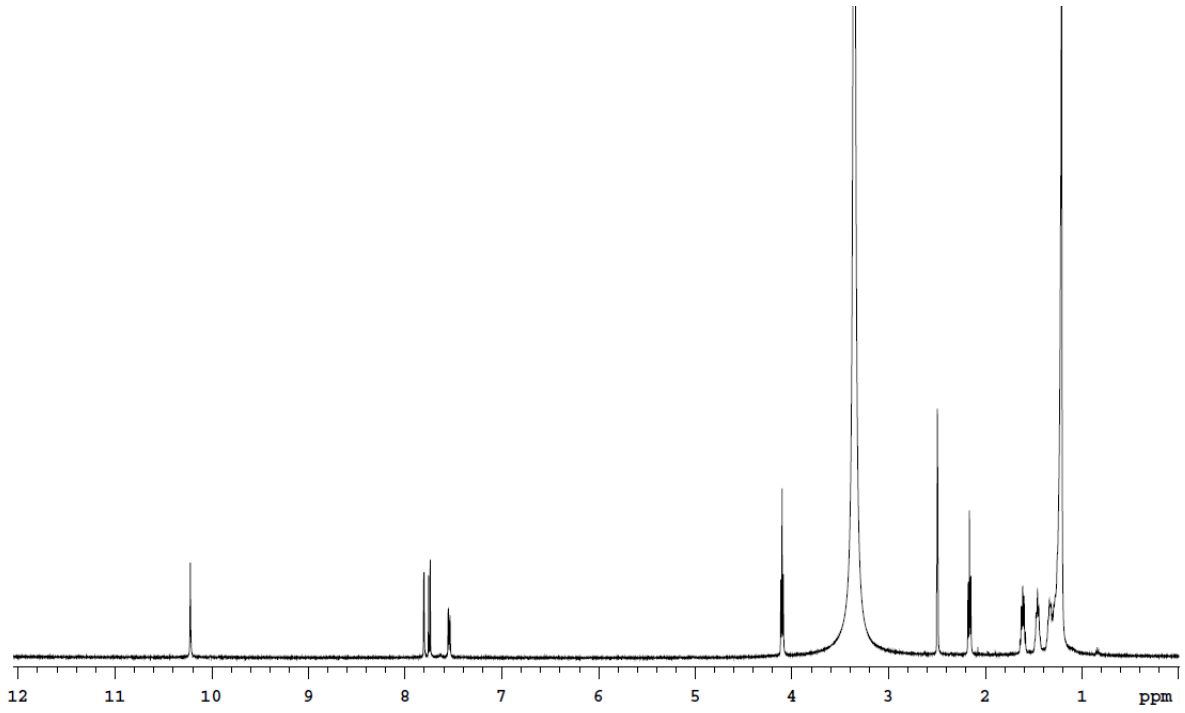

^{13}C NMR spectrum of **C2** (125 MHz, DMSO-d_6)

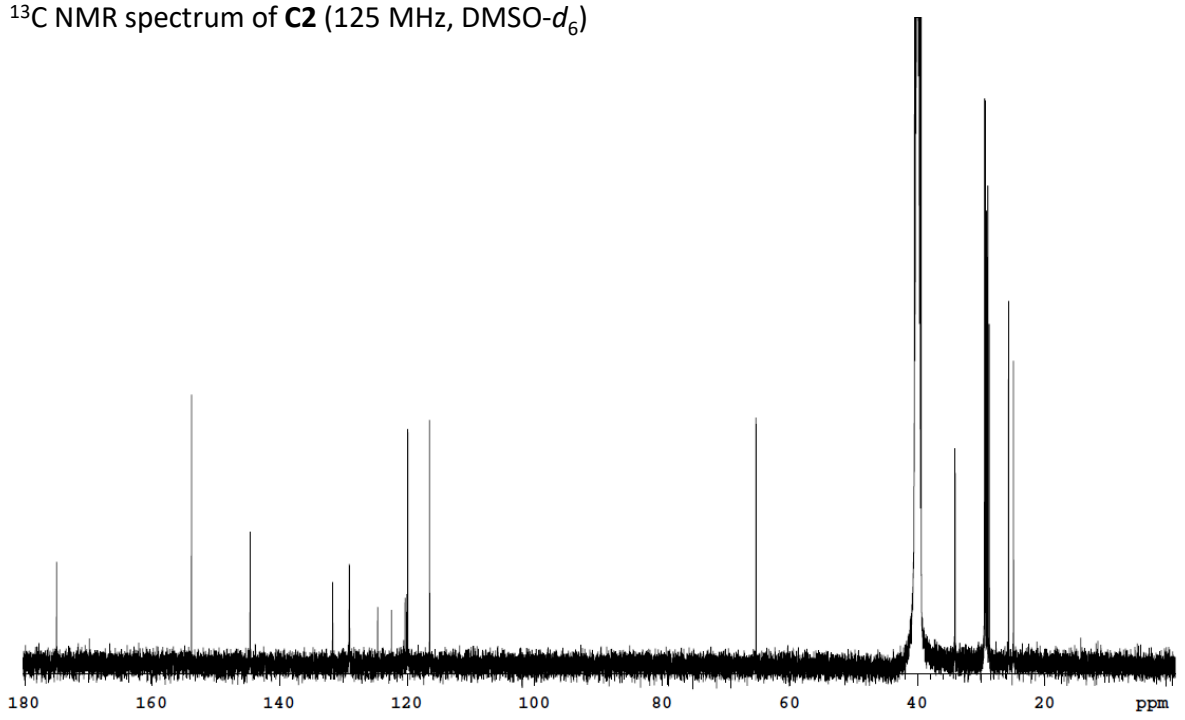

^{1}H NMR spectrum of **C3** (500 MHz, DMSO-d_6)

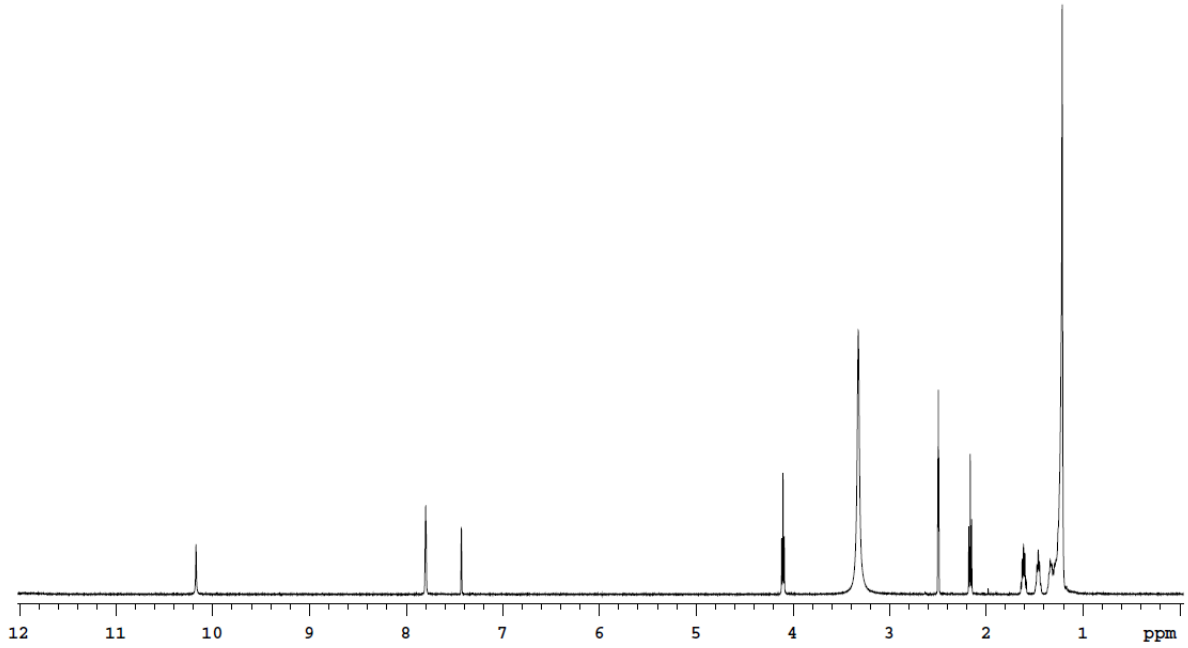

^{13}C NMR spectrum of **C3** (125 MHz, DMSO-d_6)

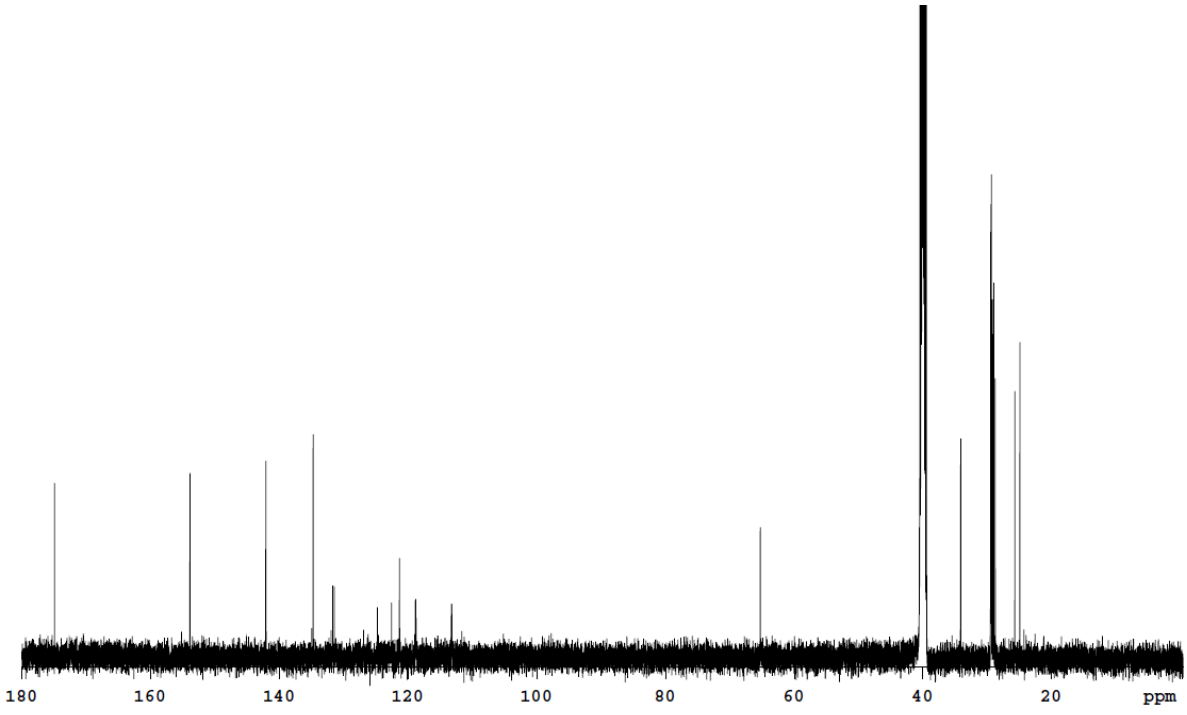

^{1}H NMR spectrum of **C4** (500 MHz, DMSO-d_6)

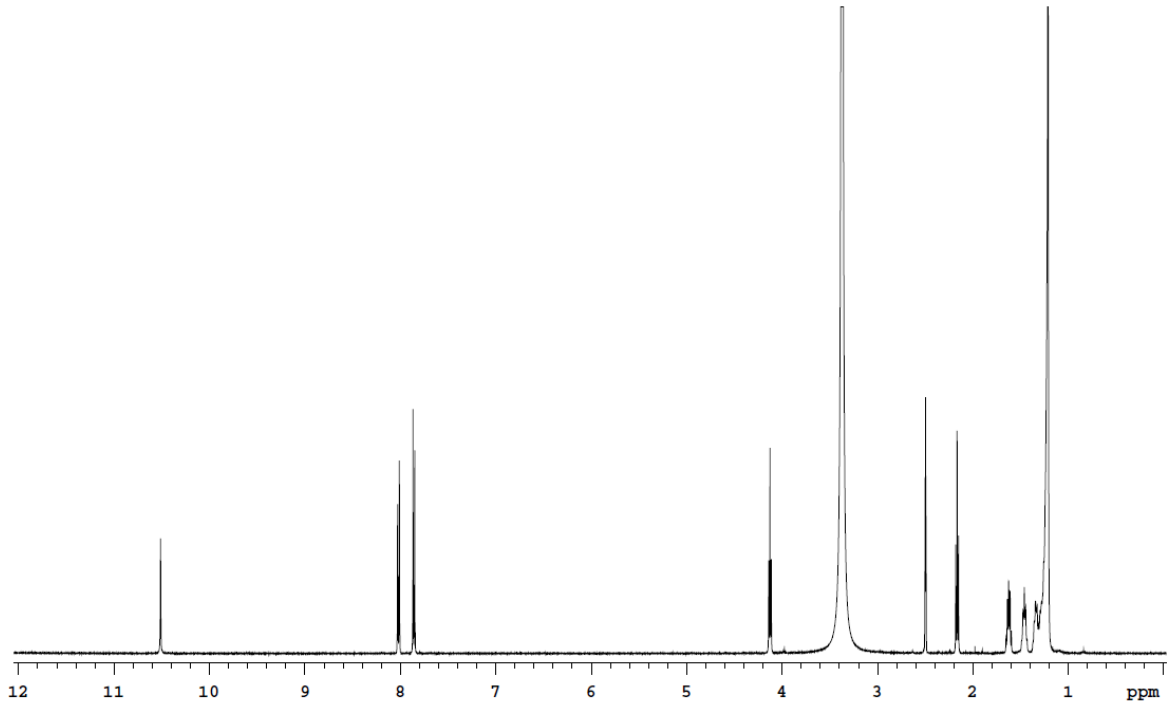

^{13}C NMR spectrum of **C4** (125 MHz, DMSO-d_6)

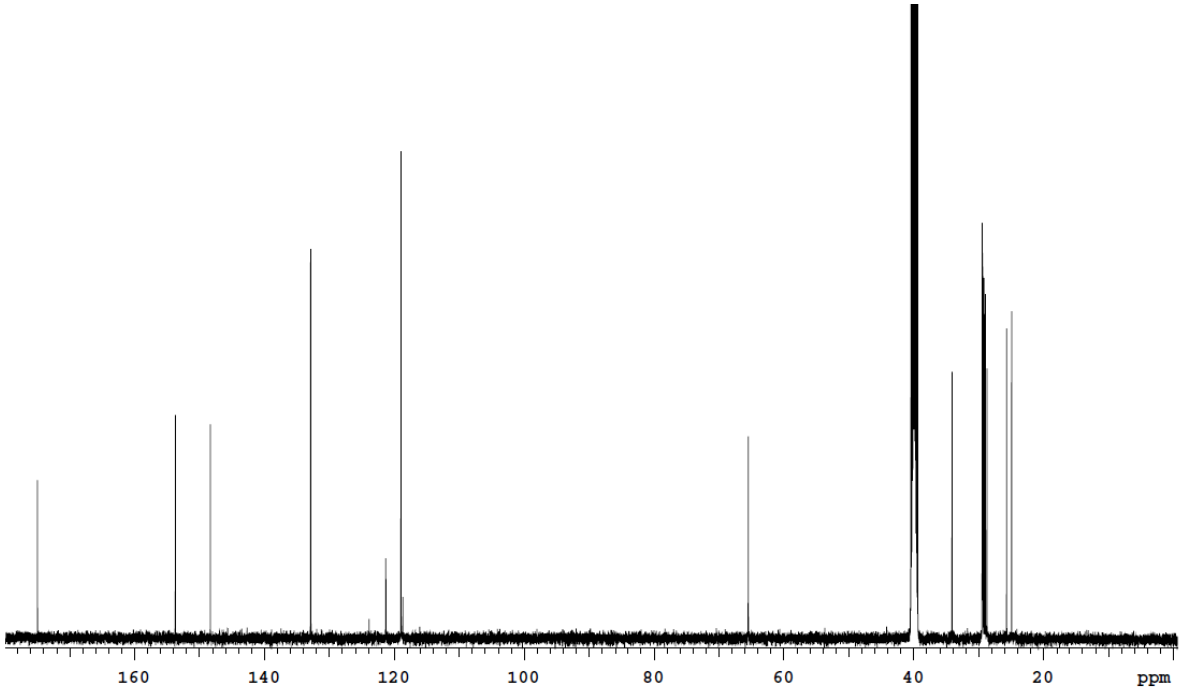

^{1}H NMR spectrum of **C5** (500 MHz, DMSO-d_6)

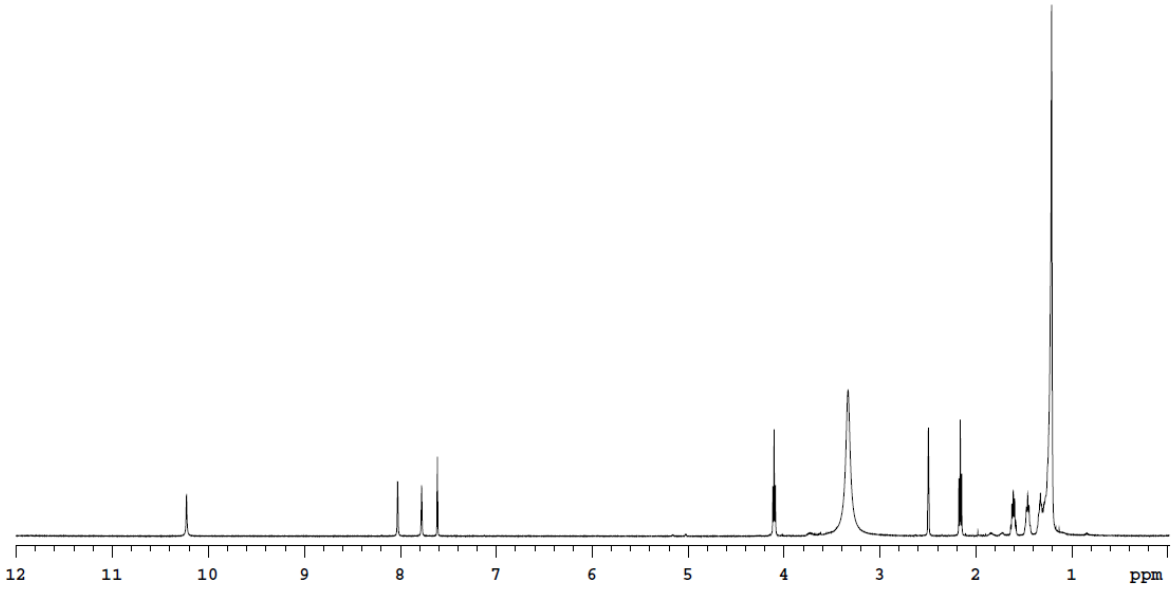

^{13}C NMR spectrum of **C5** (125 MHz, DMSO-d_6)

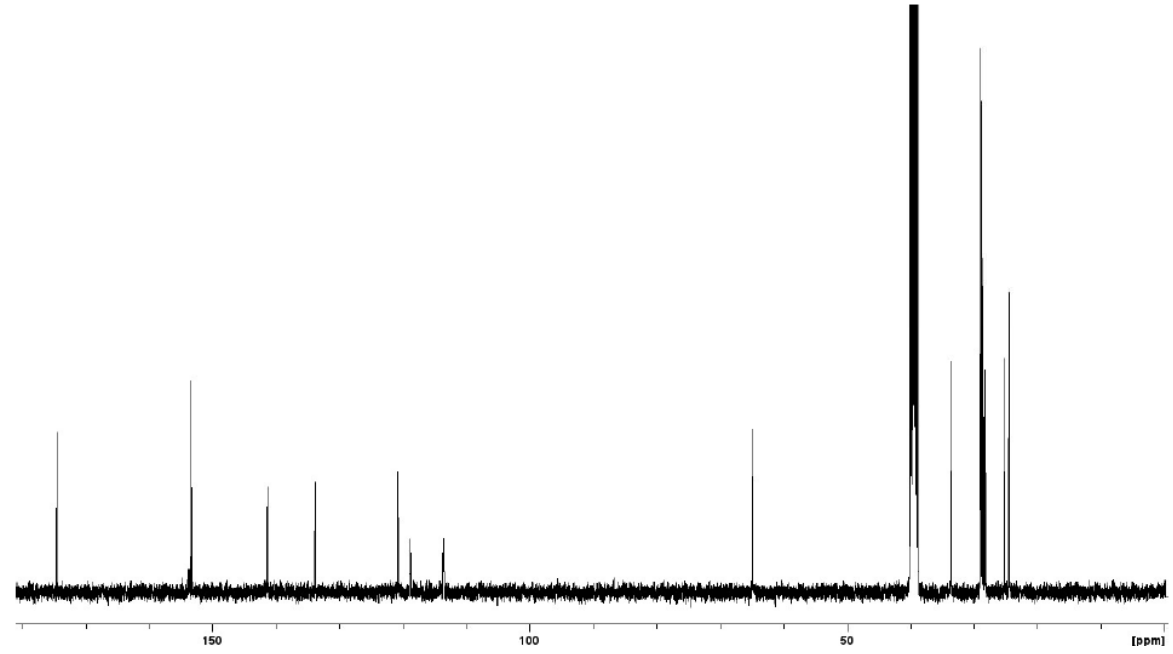

^{1}H NMR spectrum of **C6** (500 MHz, DMSO-d_6)

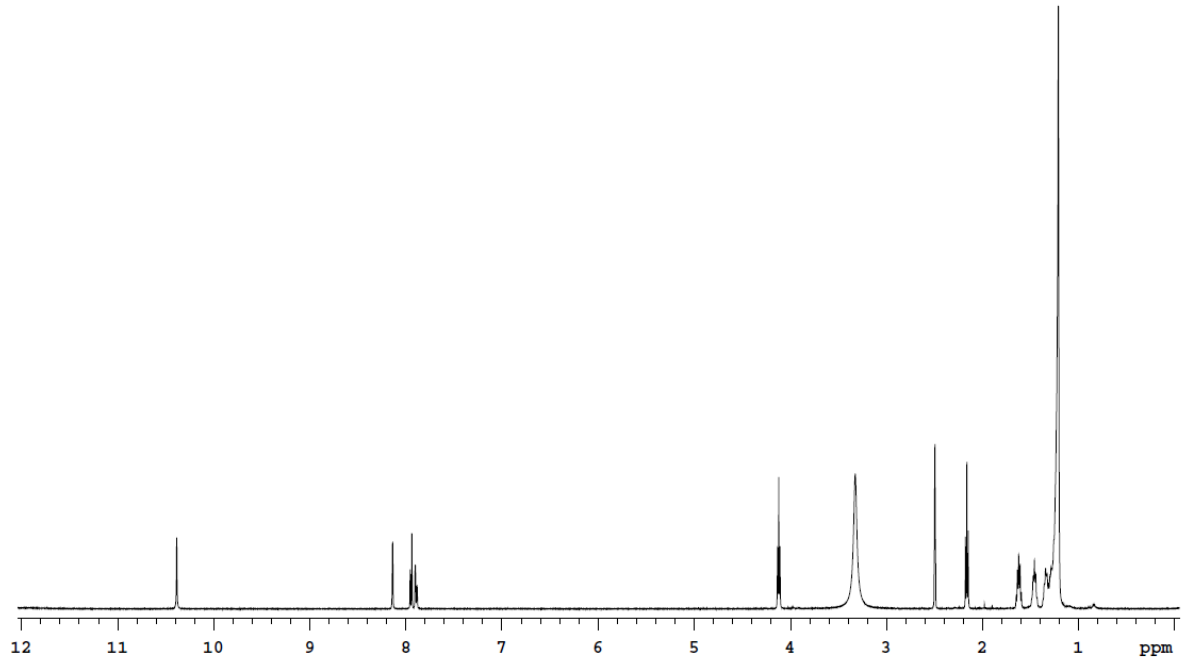

^{13}C NMR spectrum of **C6** (125 MHz, DMSO-d_6)

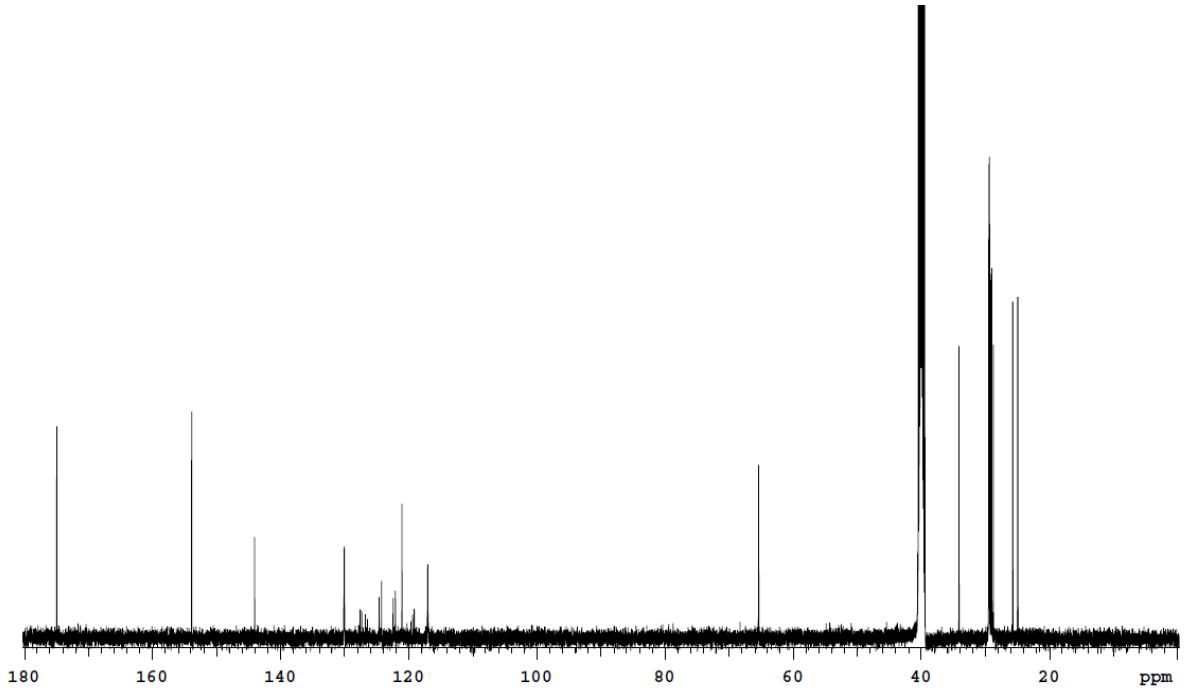

8. Additional DFT data

Table S5: Components of propanoate binding enthalpies shown in Table S2 at the DSD-PBE-P86/aug-cc-pVTZ//M06-2X-D3(0)/6-311+G(d) level of theory.

Name	M062X-D3(0)/6-311+G* Gas (hartree)	M062X-D3(0)/6-311+G* SMD Water (hartree)	M062X-D3(0)/6-311+G* SMD Pentadecane (hartree)	DSDPBEP86/aug-cc-pVTZ Gas (hartree)	DGSolv water (kJ/mol)	DGSolv Pentadecane (kJ/mol)	ZPVE (kJ/mol)	TC (kJ/mol)	S (kJ/mol/K)	TS 298.15 K (kJ/mol)	GSoln Gas (kJ/mol)	GSoln Water (kJ/mol)	GSoln Pentadecane (kJ/mol)
Propanoate	-267.800766	-267.915303	-267.848895	-267.493386	-300.72	-126.36	204.02	17.07	0.32	95.49	-702,170.36	-702,471.08	-702,296.73
C1	-1,390.671285	-1,390.680897	-1,390.683141	-1,389.323948	-25.24	-31.13	564.39	48.51	0.62	184.51	-3,647,233.70	-3,647,258.94	-3,647,264.83
C2	-1,390.672502	-1,390.682240	-1,390.684434	-1,389.325071	-25.57	-31.33	564.84	48.25	0.59	175.47	-3,647,227.43	-3,647,253.00	-3,647,258.76
C3	-1,390.675075	-1,390.683921	-1,390.686842	-1,389.328069	-23.23	-30.89	564.08	48.69	0.61	182.62	-3,647,242.76	-3,647,265.99	-3,647,273.66
C4	-1,479.610649	-1,479.629032	-1,479.624036	-1,478.169840	-48.27	-35.15	617.30	54.04	0.64	190.04	-3,880,445.68	-3,880,493.95	-3,880,480.83
C5	-1,950.292450	-1,950.301064	-1,950.303512	-1,948.610813	-22.62	-29.04	571.01	54.19	0.63	188.69	-5,115,633.26	-5,115,655.88	-5,115,662.31
C6	-1,268.121352	-1,268.130237	-1,268.131734	-1,266.751776	-23.33	-27.26	603.85	53.98	0.63	188.33	-3,325,379.36	-3,325,402.69	-3,325,406.62
C1_Propanoate	-1,658.528379	-1,658.607103	-1,658.569552	-1,656.872998	-206.69	-108.10	771.27	67.18	0.77	229.08	-4,349,502.76	-4,349,709.45	-4,349,610.86
C2_Propanoate	-1,658.530186	-1,658.611273	-1,658.571215	-1,656.874757	-212.89	-107.72	771.84	66.64	0.76	226.78	-4,349,505.05	-4,349,717.94	-4,349,612.77
C3_Propanoate	-1,658.530645	-1,658.613393	-1,658.572115	-1,656.876033	-217.25	-108.88	769.86	67.30	0.77	229.80	-4,349,512.73	-4,349,729.99	-4,349,621.61
C4_Propanoate	-1,747.472309	-1,747.556469	-1,747.512967	-1,745.723673	-220.96	-106.75	824.32	72.24	0.81	240.30	-4,582,733.32	-4,582,954.28	-4,582,840.07
C5_Propanoate	-2,218.152811	-2,218.230223	-2,218.192247	-2,216.161952	-203.24	-103.54	776.36	73.04	0.81	240.43	-5,817,916.30	-5,818,119.55	-5,818,019.84
C6_Propanoate	-1,535.981767	-1,536.059527	-1,536.020120	-1,534.303688	-204.16	-100.70	811.00	71.89	0.80	238.22	-4,027,661.74	-4,027,865.90	-4,027,762.44
U1	-1,370.794437	-1,370.814853	-1,370.811487	-1,369.461805	-53.60	-44.76	595.78	49.56	0.61	180.96	-3,595,049.67	-3,595,103.27	-3,595,094.43
U2	-1,370.796403	-1,370.816409	-1,370.812945	-1,369.463720	-52.53	-43.43	595.84	49.50	0.60	178.84	-3,595,052.57	-3,595,105.10	-3,595,096.00
U3	-1,370.799175	-1,370.818113	-1,370.815398	-1,369.466869	-49.72	-42.59	595.43	49.93	0.62	185.45	-3,595,067.44	-3,595,117.16	-3,595,110.03
U4	-1,459.735052	-1,459.763523	-1,459.752925	-1,458.308855	-74.75	-46.93	648.29	55.37	0.65	193.35	-3,828,271.66	-3,828,346.41	-3,828,318.59
U5	-1,930.416873	-1,930.435510	-1,930.432407	-1,928.749778	-48.93	-40.78	602.28	55.50	0.65	192.95	-5,063,459.79	-5,063,508.72	-5,063,500.57
U6	-1,248.245731	-1,248.264510	-1,248.260582	-1,246.890802	-49.30	-38.99	635.27	55.19	0.64	191.02	-3,273,204.44	-3,273,253.74	-3,273,243.43

U1_Propanoate	-1,638.674063	-1,638.745992	-1,638.714477	-1,637.032999	-188.85	-106.11	806.01	67.20	0.76	225.44	-4,297,374.44	-4,297,563.29	-4,297,480.55
U2_Propanoate	-1,638.677294	-1,638.747783	-1,638.717429	-1,637.035971	-185.07	-105.37	805.79	67.14	0.76	225.29	-4,297,382.37	-4,297,567.44	-4,297,487.75
U3_Propanoate	-1,638.678397	-1,638.749419	-1,638.718523	-1,637.037697	-186.47	-105.35	805.21	67.54	0.77	229.73	-4,297,391.53	-4,297,578.00	-4,297,496.89
U4_Propanoate	-1,727.620861	-1,727.695463	-1,727.660100	-1,725.886146	-195.87	-103.02	858.33	72.98	0.81	242.28	-4,530,617.12	-4,530,812.99	-4,530,720.14
U5_Propanoate	-2,198.300490	-2,198.367258	-2,198.338627	-2,196.323448	-175.30	-100.13	811.35	73.27	0.80	239.14	-5,765,793.80	-5,765,969.10	-5,765,893.92
U6_Propanoate	-1,516.128017	-1,516.196061	-1,516.166058	-1,514.464354	-178.65	-99.88	844.37	72.88	0.80	237.73	-3,975,538.72	-3,975,717.37	-3,975,638.59